View Article Online
View Journal

Dalton Transactions

An international journal of inorganic chemistry

Accepted Manuscript

This article can be cited before page numbers have been issued, to do this please use: G. B. Shul'pin, A. R. Fernandes, K. Erfurt, S. Kula, L. S. Shul'pina, Y. N. Kozlov, R. Kruszyski, B. Machura, K. A. Choroba and L. R. Raposo, *Dalton Trans.*, 2019, DOI: 10.1039/C9DT01922G.

ROYAL SOCIETY OF CHEMISTRY

rsc.li/dalton

View Article Online
DOI: 10.1039/C9DT01922G

Dalton Transactions

PAPER

View Article Online
View Journal | View Issue

Copper(II) complexes with 2,2':6',2''-terpyridine, 2,6-di(thiazol-2-yl)pyridine and 2,6-di(pyrazin-2-yl)pyridine substituted with quinolines. Synthesis, structure, antiproliferative activity, and catalytic activity in oxidation of alkanes and alcohols with peroxides †

Katarzyna Choroba,[a] Barbara Machura,*[a] Slawomir Kula,[a] Luis R. Raposo,[b] Alexandra R. Fernandes,*[b] Rafal Kruszynski,[c] Karol Erfurt,[d] Lidia S. Shul'pina,[e] Yuriy N. Kozlov [f,e] and Georgiy B. Shul'pin *[f,g,h]

[a] *Institute of Chemistry, University of Silesia, Szkolna 9, 40-006 Katowice, Poland.*

[b] *UCIBIO, Departamento de Ciências da Vida, Faculdade de Ciências e Tecnologia, Universidade NOVA de Lisboa, Campus de Caparica, 2829-516 Caparica, Portugal.*

[c] *Institute of General and Ecological Chemistry, Lodz University of Technology, Zeromskiego 116, 90-924 Lodz, Poland*

[d] *Department of Chemical Organic Technology and Petrochemistry, Silesian University of Technology, Krzywoustego 4, 44-100 Gliwice, Poland*

[e] *Nesmeyanov Institute of Organoelement Compounds, Russian Academy of Sciences, ulitsa Vavilova, dom 28, Moscow 119991, Russia*

[f] *Semenov Institute of Chemical Physics, Russian Academy of Sciences, ulitsa Kosygina, dom 4, Moscow 119991, Russia.*

[g] *Plekhanov Russian University of Economics, Stremyannyi pereulok, dom 36, Moscow 117997, Russia*

[h] *People's Friendship University of Russia, ul. Miklukho-Maklaya, dom 6, Moscow 117198, Russia*

† Electronic supplementary information (ESI) available. CCDC 1914390–1914395. For ESI and crystallographic data in CIF or other electronic format see DOI: xxxxx

orcid.org/0000-0002-1448-9228 (Shulpina)
orcid.org/0000-0002-7053-4812 (Shulpin)
orcid.org/0000-0003-0168-5753 (Choroba)
orcid.org/0000-0001-7688-6491 (Machura)
orcid.org/0000-0003-4520-1570 (Kula)

* Corresponding authors. Tel.: +7 495 7118443; fax: +7495 6512191 (GBS). E-mail addresses: shulpin@chph.ras.ru (GBS), ma.fernandes@fct.unl.pt (AF), bmachura@poczta.onet.pl (BM).

Keywords:

View Article Online
DOI: 10.1039/C9DT01922G

Alkanes
Complexes of copper
Functionalization of CH bonds
Hydroxyl radicals
Antiproliferative properties
Anti-cancer drugs

Highlights

- A series of 2,2':6',2"-terpyridine, 2,6-di(thiazol-2-yl)pyridine and 2,6-di(pyrazin-2-yl)pyridine derivatives with n-quinolyl substituents (n = 2 and 4) was used to synthetize five-coordinate complexes.
- The obtained compounds were studied as anticancer agents against human colorectal (HCT116) and ovarian (A2780) carcinoma.
- The complexes are good catalysts in oxidation of alkanes with H_2O_2 and of 1-phenylethanol with *tert*-butyl hydroperoxide in acetonitrile.
- The complexes exhibited unusual selectivity in competitive oxidation of cyclohexane and acetonitrile.
- Hydroxyl radicals take part in the reaction.

<Abstract:> A series of 2,2':6',2"-terpyridine, 2,6-di(thiazol-2-yl)pyridine and 2,6-di(pyrazin-2-yl)pyridine derivatives with n-quinolyl substituents (n = 2 and 4) was used to synthesize five-coordinate complexes $[CuCl_2(\kappa^3\text{-L})]$. The main emphasis of the research was put to investigate the impact of the triimine skeleton (*terpy*, *dtpy* and *dppy*) and n-quinolyl pendant substituent on the antiproliferative and catalytic properties of $[CuCl_2(\kappa^3\text{-L})]$. The obtained Cu(II) compounds were studied as antiproliferative agents against human colorectal (HCT116) and ovarian (A2780) carcinoma and they were used as catalysts for the oxidation of alkanes and alcohols with peroxides under mild conditions. The kinetic characteristics of the oxidizing species generated by the catalytic system Cu(II) complex–H_2O_2 in CH_3CN were obtained from the dependence of the alkane oxidation rate on its initial concentration. A model of competitive interaction of hydroxyl radicals with CH_3CN and RH in the catalyst cavity has been proposed which is based on the study simultaneously of kinetics and selectivity in alkane oxidations.

1. Introduction

Copper(I) and copper(II) complexes play important role in coordination chemistry, catalysis and biochemistry (see, for example, Refs. [1-10]). In this research, three structurally related types of triimine ligands (Fig. 1), 2,2':6',2"-terpyridine, 2,6-di(thiazol-2-yl)pyridine and 2,6-di(pyrazin-2-yl)pyridine substituted with quinolines in 4'-position of the central pyridine, have been utilized to synthesize the complexes $[CuCl_2(\kappa^3\text{-L})]$, which were studied as anticancer agents against human colorectal (HCT116) and ovarian (A2780) carcinoma and were used as catalysts for the oxidation of alkanes and alcohols with peroxides under mild conditions. The main aim of the work was to explore the impact of the triimine skeleton

View Article Online
DOI: 10.1039/C9DT01922G

and n-quinolyl substituent on biological and catalytic activity of $[CuCl_2(\kappa^3\text{-L})]$. Pyridine, thiazole and pyrazine, used as perihedral rings in the employed ligands, significantly differ in σ-donor and π-acceptor properties (pK_a = 5.23, 2.52, 0.65 for pyridine, thiazole and pyrazine respectively). On the other hand, depending on the position of nitrogen atom in pendant pyridyl ring, the ligands L^1-L^6: 4'-(quinol-2-yl)-terpy, 4'-(quinol-4-yl)-terpy, 4'-(quinol-2-yl)-dtpy, 4'-(quinol-4-yl)-dtpy, 4'-(quinol-2-yl)-dppy and 4'-(quinol-4-yl)-dppy are expected to show significant difference in the dihedral angle between the plane of the central pyridine and that of the pendant substituent, due to the inter-ring H•••H repulsions and H•••N hydrogen bonds. It should be also noted that quinolines and their derivatives are well known for their antimalarial, antimycobacterial, anticancer and antiviral behaviour [11-18].

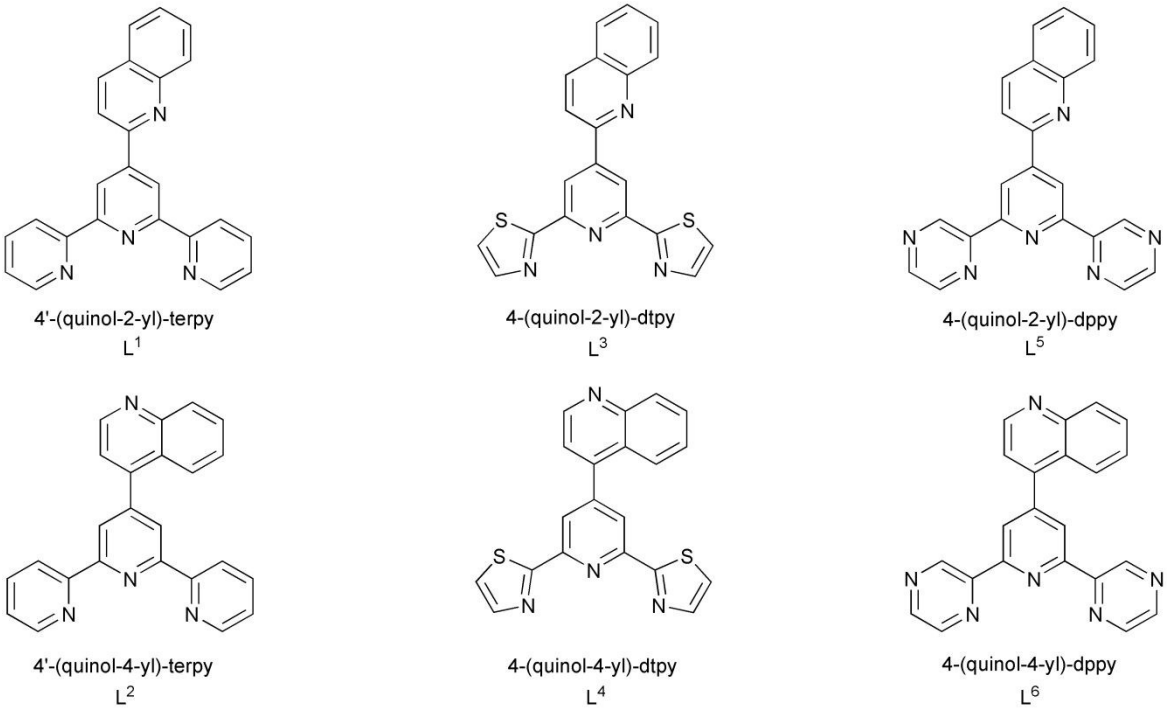

Fig. 1 2,2':6',2"-terpyridine, 2,6-di(thiazol-2-yl)pyridine (4-R-dtpy) and 2,6-di(pyrazin-2-yl)pyridine (4-R-dppy) ligands L^1-L^6 employed in this research.

Cisplatin and its analogues (carboplatin and oxaliplatin) are currently employed in the vast majority of cancer treatments, including bladder, head and neck, ovarian and testicular cancers [19-23]. The mechanism of their action involves formation of the coordination bond between the platinum(II) central ion and the nitrogen atoms at the N7 position of the guanine in the DNA helix molecule. The formed 1,2- and 1,3-intrastrand DNA cross-links induce helical stretches in DNA and transcriptional inhibition, which results in death of cancer cells via apoptosis [24-27]. Despite the clinical success of cisplatin-like drugs, however,

View Article Online
DOI: 10.1039/C9DT01922G

there is a still need for novel com pounds of antiproliferative properties and new therapeutic solutions. It is a result of severe side effects of platinum-based drugs, such as emetogenesis, neurotoxicity, myelotoxicity or nephrotoxicity as well as the emergence of tumor cells with resistance to platinum-agents [27].

Promising solutions in this field involve the development of non-platinum anticancer agents with bio-essential metal ions [28-39]. Among them, copper – the third most abundant transition metal present in the cellular body – draws special scientific attention. It serves an important role in many biological processes such as electron transfer, oxidation and dioxygen transport. Enzymes like dis-mutase have their key roles in maintaining cellular metabolic waste [40-44]. Most importantly, numerous Cu(II) compounds have been proven to be promising anticancer agents [45-50]. A remarkable anti-cancer activity was found for copper(II)–terpyridine systems [51-59]. The complexes with unsubstituted 2,2':6',2"-terpyridine ligand - $[Cu(terpy)(ClO_4)_2(H_2O)]$ and $[Cu(terpy)_2](CF_3SO_3)_2{\cdot}2H_2O$ [60], interacting with DNA via major groove were found to display significant antiproliferative activity against non-small cell lung cancer cell line (A549). The vast majority of 4'-substituted terpyridine copper(II) coordination compounds bind to double helix DNA through intercalation, and their cytotoxicity behavior is strongly dependent on the substituent introduced into 2,2':6',2"-terpyridine moiety, which affect the geometry of the coordination compound and controls self-assembly processes. The enhanced antiproliferative activity, higher in comparison with cisplatin, was reported for $[Cu(Anth\text{-}terpy)_2](ClO_4)_2$ against the cancer cell lines MCF-7, HepG2, H1299, HeLa, SiHa and Ca Ski [61].

It should be also noted that copper complexes and among them copper-containing terpy compounds are of a high potential interest as catalysts, especially in oxidation processes [62-65]. These complexes contain the so-called redox ligands [66-70]. Noncovalent interactions play important role in catalysis.[71,72]

2. Experimental

2.1. Materials

The salt $CuCl_2{\cdot}2H_2O$ used in the synthesis was commercially available and was used without further purification. Ligands L^1-L^6 were prepared according to the modified method employed in our previous studies [73-75]. All solvents for the synthesis of the ligands and complexes were of reagent grade and were used as received.

2.2. Instrumentation

The IR spectra were recorded using a Nicolet iS5 spectrophotometer in the range 4000-400 cm^{-1} with the samples in the form of KBr pellets. The electronic spectra were obtained using Nicolet Evolution

View Article Online
DOI: 10.1039/C9DT01922G

220 in the spectral range 210–1000 nm in methanol and in the spectral range 190–1100 nm in the solid state.

2.3. X-ray crystallographic analysis

The X-ray diffraction data was collected on Oxford Diffraction four-circle diffractometer Gemini A Ultra with Atlas CCD detector using graphite monochromated Mo Ka radiation (λ = 0.71073 Å) at room temperature. Details concerning crystal data and refinement are given in Table 1. Diffraction data collection, cell refinement and data reduction. were performed using the CrysAlis^{Pro} software [76]. The structures were solved by the Patterson method using SHELXS97 and refined by full-matrix least-squares on F^2 using SHELXL97 [77,78]. All the non-hydrogen atoms were refined anisotropically, and hydrogen atoms were placed in calculated positions refined using idealized geometries (riding model) and assigned fixed isotropic displacement parameters, d(C–H) = 0.93 Å, U_{iso}(H) = 1.2 U_{eq}(C) (for aromatic) and d(C–H) = 0.96 Å, U_{iso}(H) = 1.5 U_{eq}(C) (for methyl) and U_{iso}(H) = 1.5 U_{eq}(O) (for water). The methyl groups were allowed to rotate about their local threefold axis. The water solvent molecule of compound **5** is disordered over two positions with the 14:11 participation of the disordered domains.

Table 1 Crystal data and structure refinement for copper(II) compounds.

View Article Online
DOI: 10.1039/C9DT01922G

Complex	**(1)**	**(2)**	**(3)**	**(4)**	**(5)**	**(6)**
used ligand	**4'-(2-quinoline)-terpy**	**4'-(4-quinoline)-terpy**	**4'-(2-quinoline)-dtpy**	**4'-(4-quinoline)-dtpy**	**4'-(2-quinoline)-dppy**	**4'-(4-quinoline)-dppy**
Empirical formula	$C_{24}H_{16}Cl_2CuN_4$	$C_{24}H_{16}Cl_2CuN_4$	$C_{20}H_{12}Cl_2CuN_4S_2$	$C_{20}H_{18}Cl_2CuN_4O_3S_2$	$C_{22}H_{16}Cl_2CuN_6O$	$C_{23}H_{18}Cl_2CuN_6O$
Formula weight	494.85	494.85	506.90	560.94	514.85	528.87
Temperature [K]	295.0(2)	295.0(2)	295.0(2)	295.0(2)	295.0(2)	295.0(2)
Wavelength [Å]	0.71073	0.71073	0.71073	0.71073	0.71073	0.71073
Crystal system	Monoclinic	Monoclinic	Orthorhombic	Triclinic	Monoclinic	Triclinic
Space group	$P2_1/c$	$P2_1/n$	$Pna2_1$	P-1	I2/a	P-1
Unit cell dimensions [Å,°]	a = 7.7287(3)	a = 7.9474(5)	a = 23.3543(15)	a = 7.8923(5)	a = 13.4958(6)	a = 7.8743(3)
	b = 14.2823(7)	b = 22.7151(11)	b = 11.0536(6)	b = 11.31080(10)	b = 12.6508(6)	b = 10.5456(7)
	c = 18.7465(9)	c = 11.6628(6)	c = 7.7194(4)	c = 13.6000(14)	c = 25.5678(10)	c = 13.8368(9)
	α = 90	α = 90	α = 90	α = 71.716(9)	α = 90	α = 97.810(5)
	β = 97.268(4)	β = 92.888(6)	β = 90	β = 74.885(7)	β = 101.202(5)	β = 96.724(4)
	γ = 90	γ = 90	γ = 90	γ = 87.322(6)	γ = 90	γ = 93.962(4)
Volume [Å^3]	2052.68(16)	2102.8(2)	1992.8(2)	1112.06(15)	4282.1(3)	1126.28(11)
Z	4	4	4	2	8	2
Density (calculated) [Mg/m^3]	1.601	1.563	1.690	1.675	1.597	1.559
Absorption coefficient [mm^{-1}]	1.345	1.313	1.589	1.442	1.298	1.236
F(000)	1004	1004	1020	570	2088	538
Crystal size [mm]	0.58 × 0.23 × 0.08	0.19 × 0.07 × 0.04	0.21 × 0.04 × 0.04	0.19 × 0.05 × 0.02	0.14 x 0.08 x 0.07	0.32 × 0.15 × 0.04
θ range for data collection [°]	3.32 to 25.05	3.30 to 25.05	3.49 to 25.05	3.48 to 25.05	3.43 to 25.05	3.33 to 25.04
Index ranges	-9≤ h ≤8	-9≤ h ≤7	-27≤ h ≤23	-9≤ h ≤9	-16≤ h ≤15	-9≤ h ≤9
	-16≤ k ≤17	-27≤ k ≤23	-13≤ k ≤11	-13≤ k ≤13	-14≤ k ≤15	-12≤ k ≤12
	-21≤ l≤22	-13≤ l≤13	-9≤ l≤7	-12≤ l≤16	-25≤ l≤30	-16≤ l≤16
Reflections collected	9696	8451	8115	8252	9458	10462
Independent reflections	3624 (R_{int} = 0.0297)	3711 (R_{int} = 0.0541)	2947 (R_{int} = 0.0286)	3779 (R_{int} = 0.0698)	3771 (R_{int} = 0.0214)	3993 (R_{int} = 0.0298)
Completeness to 2theta	99.8%	99.8%	99.6%	95.7%	99.7%	99.8%
Min. and max. transm.	0.848 and 1.000	0.609 and 1.000	0.759 and 1.000	0.764 and 1.000	0.783 and 1.000	0.813 and 1.000
Data / restraints / parameters	3624 / 0 / 280	3711 / 0 / 280	2947 / 1 / 262	3779 / 0 / 298	3771 / 0 / 299	3993 / 0 / 300
Goodness-of-fit on F^2	1.026	1.069	1.046	1.033	1.077	1.049
Final R indices [I>2σ(I)]	R1 = 0.0323	R1 = 0.0629	R1 = 0.0284	R1 = 0.0490	R1 = 0.0357	R1 = 0.0328
	wR2 = 0.0725	wR2 = 0.1201	wR2 = 0.0609	wR2 = 0.1171	wR2 = 0.0876	wR2 = 0.0759
R indices (all data)	R1 = 0.0466	R1 = 0.1058	R1 = 0.0338	R1 = 0.0794	R1 = 0.0485	R1 = 0.0439
	wR2 = 0.0776	wR2 = 0.1310	wR2 = 0.0640	wR2 = 0.1470	wR2 = 0.0926	wR2 = 0.0810
Largest diff. peak and hole [e Å^{-3}]	0.22 and -0.34	0.59 and -0.44	0.31 and -0.27	0.58 and -0.76	0.58 and -0.31	0.25 and -0.34
CCDC number	1914390	1914391	1914392	1914393	1914394	1914395

2.4. Synthesis of the complexes

General synthesis of [$CuCl_2$(R^n-terpy)], [$CuCl_2$(R^n-dtpy)] and [$CuCl_2$(R^n-dppy)] (1-6).

The salt $CuCl_2{\cdot}2H_2O$ (0.17 g, 1 mmol) dissolved in methanol (10 ml) was added dropwise to a hot methanolic solution of the corresponding L^n (1 mmol). The resulting solution was stirred at room temperature for 2 h, and after a few days green crystalline solids were precipitated. Single crystals of [Cu(L^n)Cl_2] with ligands L^1-L^4 suitable for X-ray were obtained directly from the mother liquor. To obtain single crystals of [Cu(L^n)Cl_2] with 2,6-di(pyrazin-2-yl)pyridine ligands (L^5 and L^6) slow diffusion technique in a H-tube was used. The one arm of the H-tube was filled with a methanolic solution of $CuCl_2{\cdot}2H_2O$, while a CH_2Cl_2/CH_3OH solution of the appropriate ligand L^5 or L^6 was placed in the other arm of the H-tube. The

View Article Online
DOI: 10.1039/C9DT01922G

H-tubes were allowed to stand for a period of about two weeks, and well-shaped X-quality crystals of **5** and **6** were obtained.

[$CuCl_2(L^1)$] (1): Yield 55%. HRMS (ESI): calcd for $C_{24}H_{16}N_4ClCu^+$ 458.0359 found 458.0359. IR (KBr, cm^{-1}): 3055 (m), 3018 (m), 1611 (s), 1568 (m), 1552 (m), 1508 (m), 1475 (s), 1438 (m), 1416 (m), 1380 (w), 1336 (m), 1304 (w), 1248 (m), 1160 (m), 1125 (w), 1033 (m), 1019 (m), 902 (w), 893 (w), 835 (m), 802 (m), 790 (s), 747 (m), 728 (w), 690 (m), 656 (m), 645 (m), 623 (w), 569 (w), 480 (w), 418 (w). UV-Vis (MeOH, λ_{max}, nm ($\varepsilon \cdot 10^4$, $dm^3 \cdot mol^{-1} \cdot cm^{-1}$)): 216 (4.78), 226 (5.48), 276 (3.99), 330 (2.89), 701 (0.01). UV-Vis (solid, nm): 232, 283, 331, 423, 753.

[$CuCl_2(L^2)$] (2): Yield 50%. HRMS (ESI): calcd for $C_{24}H_{16}N_4ClCu^+$ 458.0359 found 458.0359. IR (KBr, cm^{-1}): 3062 (m), 3014 (m), 1616 (s), 1603 (m), 1588 (m), 1567 (m), 1555 (s), 1509 (m), 1477 (s), 1447 (w), 1428 (m), 1412 (m), 1391 (w), 1362 (w), 1306 (m), 1288 (w), 1248 (m), 1220 (w), 1207 (w), 1161 (m), 1129 (w), 1048 (w), 1035 (m), 1018 (m), 923 (m), 874 (w), 855 (w), 846 (w), 808 (m), 795 (m), 767 (s), 737 (w), 671 (m), 646 (m), 623 (m), 425 (w). UV-Vis (MeOH, λ_{max}, nm ($\varepsilon \cdot 10^4$, $dm^3 \cdot mol^{-1} \cdot cm^{-1}$)): 216 (5.12), 224 (5.38), 263 (2.71), 287 (2.06), 328 (1.65), 340 (1.51), 703 (0.01). UV-Vis (solid, nm): 227, 291, 329, 680, 747.

[$CuCl_2(L^3)$] (3): Yield 70%. HRMS (ESI): calcd for $C_{20}H_{12}N_4S_2ClCu^+$ 469.9488 found 469.9488. IR (KBr, cm^{-1}): 3107 (w), 3069 (m), 2988 (m), 1846 (w), 1793 (w), 1668 (w), 1608 (s), 1591 (m), 1548 (m), 1508 (m), 1494 (m), 1480 (s), 1452 (s), 1437 (m), 1426 (m), 1379 (m), 1356 (m), 1336 (m), 1314 (m), 1280 (w), 1248 (m), 1232 (m), 1214 (m), 1191 (s), 1158 (w), 1143 (w), 1123 (w), 1086 (m), 1023 (m), 928 (w), 899 (m), 888 (w), 839 (s), 790 (s), 773 (s), 759 (s), 741 (m), 697 (w), 642 (m), 621 (w), 595 (m), 573 (w), 514 (w), 474 (w). UV-Vis (MeOH, λ_{max}, nm ($\varepsilon \cdot 10^4$, $dm^3 \cdot mol^{-1} \cdot cm^{-1}$)): 213 (3.47), 230 (3.33), 282 (3.03), 307 (2.68), 333 (2.38), 372 (1.02), 748 (0.008). UV-Vis (solid, nm): 228, 279, 333, 383, 814.

[$CuCl_2(L^4)$] (4): Yield 65%. HRMS (ESI): calcd for $C_{20}H_{12}N_4S_2ClCu^+$ 469.9488 found 469.9490. IR (KBr, cm^{-1}): 3421 (m), 3028 (m), 1609 (s), 1584 (m), 1567 (w), 1549 (m), 1509 (w), 1494 (m), 1482 (s), 1446 (s), 1422 (m), 1350 (m), 1302 (w), 1245 (m), 1198 (s), 1127 (w), 1077 (w), 1026 (w), 892 (w), 877 (w), 866 (w), 855 (w), 791 (s), 744 (m), 720 (w), 679 (w), 630 (m), 615 (m), 594 (w), 443 (w), 424 (w). UV-Vis (MeOH, λ_{max}, nm ($\varepsilon \cdot 10^4$, $dm^3 \cdot mol^{-1} \cdot cm^{-1}$)): 214 (4.46), 224 (4.24), 253 (2.05),

View Article Online
DOI: 10.1039/C9DT01922G

278 (2.43), 304 (2.33), 346 (1.55), 364 (1.17), 745 (0.008). UV-Vis (solid, nm): 230, 278, 331, 402, 787.

[$CuCl_2(L^5)$] (5): Yield 90%. HRMS (ESI): calcd for $C_{22}H_{14}ClCuN_6^+$ 460.0264 found 460.0271. IR (KBr, cm^{-1}): 3576 (w), 3472 (m), 3042 (w), 1608 (s), 1591 (m), 1550 (m), 1508 (m), 1470 (w), 1454 (m), 1436 (m), 1418 (w), 1394 (m), 1377 (m), 1359 (w), 1336 (w), 1314 (w), 1293 (w), 1233 (w), 1181 (s), 1146 (m), 1082 (w), 1039 (s), 1025 (m), 945 (w), 901 (m), 856 (m), 841 (s), 792 (w), 785 (w), 770 (m), 720 (m), 691 (w), 685 (w), 621 (w), 568 (w), 518 (w), 475 (m), 414 (m). UV-Vis (MeOH, λ_{max}, nm ($\varepsilon \cdot 10^4$, $dm^3 \cdot mol^{-1} \cdot cm^{-1}$)): 213 (2.95), 224 (2.90), 286 (2.02), 339 (1.66), 355 (1.31), 745 (0.006). UV-Vis (solid, nm): 230, 278, 330, 392, 450, 777.

[$CuCl_2(L^6)$] (6): Yield 95%. HRMS (ESI): calcd for $C_{22}H_{14}ClCuN_6^+$ 460.0264 found 460.0267. IR (KBr, cm^{-1}): 3421 (s), 3061 (m), 1653 (w), 1615 (s), 1586 (m), 1553 (m), 1511 (w), 1477 (m), 1459 (s), 1432 (w), 1404 (m), 1383 (m), 1307 (m), 1283 (w), 1252 (w), 1185 (s), 1151 (m), 1096 (w), 1074 (w), 1039 (s), 901 (w), 868 (m), 847 (m), 767 (m), 743 (w), 689 (w), 669 (w), 627 (m), 493 (m), 428 (m). UV-Vis (MeOH, λ_{max}, nm ($\varepsilon \cdot 10^4$, $dm^3 \cdot mol^{-1} \cdot cm^{-1}$)): 216 (4.34), 226 (4.86), 276 (2.37), 338 (1.43), 350 (1.96), 735 (0.007). UV-Vis (solid, nm): 229, 275, 325, 390, 450, 750.

2.5. Biological assays

Cell culture

Cancer derived cell lines HCT116 (colorectal carcinoma) and A2780 (ovarian carcinoma) and Human normal primary fibroblasts were grown in Dulbecco's modified Eagle medium (DMEM) supplemented with 10% (v/v) fetal bovine serum (FBS) and 1% PenStrep solution (all solutions from Thermo Fischer Scientific, Waltham, MA, USA), and maintained at 37ºC in a humidified atmosphere with 5% (v/v) CO_2 as previously described [79,80, 88,89]. HCT116 and human epidermal fibroblasts from American Type Culture Collection (ATCC, Manassas, VA, USA and A2780 cell line was purchased from Merck (Darmstadt, Germany).

Determination of dose response curves - Viability assays

In 96-well plates.7500 cells/well were seeded and after 24 h, the culture media was replaced and cells incubated for another 48 h with increasing concentrations of DMSO or Cu(II) complexes bearing quinol-substituted terpy, dtpy or dppy ligands [79-81]. After this incubation, cell viability was evaluated with the

View Article Online
DOI: 10.1039/C9DT01922G

CellTiter 96® Aqueous Non-Radioactive Proliferation assay (MTS assay) (Promega, Madison, WI, USA). The dehydrogenase enzymes of viable cells (metabolically active) reduce 3-(4,5-dimethylthiazol-2-yl)-5-(3-carboxymethoxyphenyl)-2-(4-sulfophenyl)-2H-tetrazolium, inner salt (MTS), with phenazinemethosulfate (PMS), an electron coupling reagent, to form formazan that can measured. Absorbance at 490 nm in a Bio-Rad microplate reader, model 680 (Bio-Rad, Hercules, CA, USA) is used to determine the amount of formazan formed by viable cells. The quantity of formazan formed is directly proportional to viable cells. The GraphPad Prism 7.00 program (GraphPad Software, La Jolla, CA, USA) is used to determine the concentration that inhibits 50% of the cellular proliferation (IC_{50}) as compared to the respective solvent control (DMSO 0.1% v/v) using dose response curves.

Evaluation of apoptosis in HCT116 cells by fluorescence microscopy (Hoechst staining)

In 24-well plates, $3.75x10^4$ HCT116 cells were seeded per well and incubated for 24 h and then incubated for 48 h with IC_{50} concentrations of Cu(II)quinolyl-4-yl-terpy (**2)** and Cu(II)quinolyl-2yl-dppy (**5**), as previously described [82,83]. DMSO 0.1% (v/v) was used as solvent control. After the 48 h incubation, cells were washed with PBS 1X, and then fixed with 4% (w/v) paraformaldehyde and stained for 15 min with 7.5 µg/mL Hoechst 33258 (Thermo Fischer Scientific). Again, cells were washed thrice in PBS 1X and then. photographed with a Ti-U Eclipse inverted fluorescence microscope (Nikon, Tokyo, Japan) using a "DAPI" fluorescence filter cube (Nikon) and images were captured with the NIS Elements Basic software (Nikon). At least 50 nuclei from 3 random microscopic fields were scored per replicate and the condensation and fragmentation of HCT116 nuclei, were used to identify apoptotic cells.

Reactive oxygen species (ROS) production of in HCT116 cells

As previously described [82,83,84], 6-well plates with $3.75x10^4$ HCT116 cells per well were incubated with DMSO 0.1% (v/v) (vehicle control), 25 µM H_2O_2 (positive control) and IC_{50} concentrations of Cu(II)quinolyl-4-yl-terpy (**2)** and Cu(II)quinolyl-2yl-dppy (**5**) for 48 h. Then followed an incubation with 10 µM 2′,7′-dichlorodihydrofluorescein diacetate (H2DCF-DA) (ThermoFisher Scientific) for 30 min at 37 ºC. The acetate groups of the compound are removed by intracellular esterases in the presence of ROS, increasing the fluorescence of the compound. A Attune acoustic focusing cytometer (ThermoFisher Scientific) was used to measure the fluorescence of HCT116 cells and the retrieved data analyzed in the respective software (Attune Cytometric Software, vs. 2.1).

Statistical analysis

View Article Online
DOI: 10.1039/C9DT01922G

Data presented in this work are expressed as the mean±SD of at least three independent experiments. Statistical significance was determined using the Student t-test. Differences were considered significative if $p<0.05$. The GraphPad Prism v7.00 (GraphPad Software, La Jolla, CA, USA) was used to determine IC_{50} and perform statistical analysis.

2.6 Oxidation reactions

The oxidation reactions were typically carried out in air in thermostated Pyrex cylindrical vessels with vigorous stirring; total volume of the reaction solution was 2.5 mL (**CAUTION**: the combination of air or molecular oxygen and H_2O_2 with organic compounds at elevated temperatures may be explosive!). Initially, a portion of 50% aqueous solution of hydrogen peroxide or 70% aqueous *tert*-butyl hydroperoxide was added to the solution of the catalyst and substrate in acetonitrile. The reaction solutions were analyzed by GC (instruments DANI-86.10, capillary column 50 m × 0.25 mm × 0.25 μm, Carbowax 20M; the carrier gas was helium, and LKhM-80-6, columns 2 m with 5% Carbowax 1500 on 0.25–0.315 mm Inerton AW-HMDS; carrier gas was argon). Usually samples were analyzed twice, i.e. before and after the addition of the excess of solid PPh_3. This method was developed and used previously by Shul'pin [85-91]. Since alkyl hydroperoxides, which are transformed in the GC injector into a mixture of the corresponding ketone and alcohol, are quantitatively reduced with PPh_3 to give the corresponding alcohol, this method allows us to calculate the real concentrations not only of the hydroperoxide but of the alcohols and ketones present in the solution at a given moment.

3. Results and discussion

3.1 Synthesis and characterization of compounds 1-6

The quinolyl-substituted 2,2′:6′,2″-terpyridine, 2,6-di(thiazol-2-yl)pyridine and 2,6-di(pyrazin-2-yl)pyridine derivatives (Fig. 1) were synthesized according to the modified one-pot method [92,93,94] based on condensation of the corresponding aldehyde (2-quinolinylcarboxaldehyde or 4-quinolinylcarboxaldehyde) with 2-acetylpyridine, 2-acetylthiazole and 2-acetylpyrazine, respectively. The Cu(II) complexes $[Cu(L^n)Cl_2]$ were isolated as green solids by reaction of methanol solution of the appropriate quinolyl-substituted triimine ligand (L^n) with methanolic solution of $CuCl_2 \cdot 2H_2O$.

The molecular formulae of the Cu(II) complexes were determined by single crystal X-ray diffraction analysis and confirmed by high resolution mass spectrometry HR-MS (Fig. S1, ESI†). In the IR spectra, the vibrational bands $\nu_{(C=C)}$ and $\nu_{(C=N)}$ assigned to coordinated N–heterocyclic ligands are observed in the range

View Article Online
DOI: 10.1039/C9DT01922G

1608–1549 cm^{-1} (see Fig. S2, ESI†) and are slightly shifted towards higher wavenumbers compared to the free ligands.

Perspective views showing the molecular structures of **1-6** with the atom numbering are presented in Fig. 2. The selected bond distances and bond angles of **1-6** are given in Table S1, ESI†.

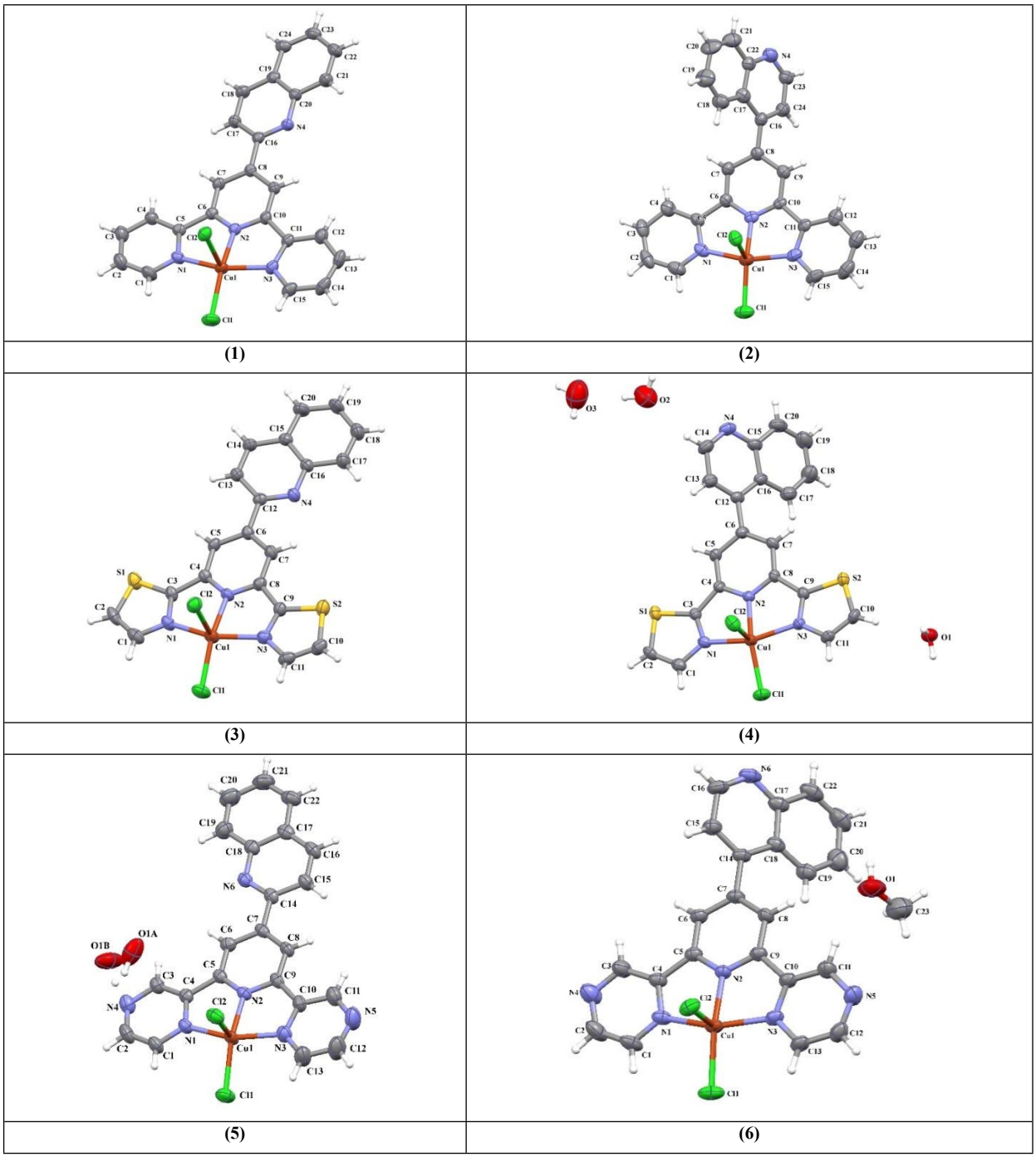

Fig. 2 Perspective views showing the molecular structures of the copper(II) complexes with the atom numbering. Displacement ellipsoids are drawn at the 50% probability level.

View Article Online
DOI: 10.1039/C9DT01922G

The copper(II) centre, coordinated to the triimine ligand (L^n) and chloride ion, displays a distorted square-pyramidal geometry. The angular structural index parameter τ, expressed as the difference between the two largest angles divided by 60 [95], adopts value close to 0, it is 0.093 for **1**, 0.056 for **2**, 0.092 for **3**, 0.003 for **4**, 0.014 for **5** and 0.090 for **6**. The deviations of N–Cu–N angles in the basal plane from the idealized values of 90° and 180° are attributed to the geometrical constraints issued from κ^3N coordination of the L^n ligand. Occurrence of the five-membered chelate rings of tridentate L^n results in N(2)–Cu(1)–N(1) and in N(2)–Cu(1)–N(3) angles falling in the range 77.90(14)°–79.71(8)°. The nitrogen N(1), N(2), N(3) and chlorine Cl(1) atoms in the basal plane are nearly coplanar within ±0.1160(11) Å for **1**, ±0.1364 (22) Å for **2,** ±0.1209(20) Å for **3,** ±0.1837(22) Å for **4,** ±0.2021(13) Å for **5** and ±0.1067(10) Å for **6**, while the copper center is displaced 0.2136(7) Å for **1**, 0.2388(15) Å for **2,** 0.2530(14) Å for **3,** 0.2876(15) Å for **4,** 0.2527(9) Å for **5** and 0.2677(7) Å for **6** from the least-squares plane towards the chloride ion in the apical site.

In analogy to the related square-pyramidal Cu(II) complexes, the Cu–N bond of the central pyridine is shorter compared to those of peripheral triimine rings, and the Cu–Cl apical bond length is longer than the Cu–Cl basal distance. The elongation of Cu(1)–Cl(2) is attributed to Jahn Teller distortion [96].

The striking difference between the Cu(II) complexes bearing quinol-2-yl substituted ligands (**1**, **3** and **5**) and those with quinol-4-yl group (**2**, **4** and **6**) concerns relative orientation of the pendant substituent and central pyridine ring. Due to the inter-ring H•••H repulsions. The quinol-4-yl unit is strongly inclined to the central pyridine at 53.96(14)° in **2**, 49.10(15)° in **4** and 52.50(6) in **6**. On the contrary, the pendant substituent of **1**, **3** and **5** is quite coplanar with the central pyridine ring, with dihedral angles of 7.91(13)° in **1**, 13.91(16)° in **3** and 4.68(8)° in **5**. In all the complexes, the triimine skeleton is approximately planar. The maximum value of the dihedral angle between the mean planes of the central pyridine and peripheral piryd-2-yl/thiazol-2-yl/pyrazin-2-yl rings was found for **6** (8.58(13)°).

A summary of the intermolecular contacts in the crystal structures **1**-**6** is given in Fig. S3 and Tables S2-S4, ESI†. Crystal packing of **4**, **5**, and **6** appears to be strongly affected by hydrogen bonds C—H•••O, O—H•••Cl and O—H•••N formed with participation of lattice solvent molecules (H_2O in **4** and **5** and MeOH in **6**). Furthermore, the reported crystal structures are stabilized by weaker C–H•••Cl, π•••π and π•••Cl interactions. Most remarkably, in the crystal lattice of **4**, the water molecules O(2)W and O(3)W are arranged into four-membered rings, as shown in Fig. 3. In each water tetramer $(H_2O)_4$, the O(2)W and O(3)W act as both hydrogen donors and acceptors molecules. The O–O–O angles are 84.0(3)° and 96.0(3)°, and the O···O separations equal to 2.761(9) Å and 2.823(9) Å. Noteworthy, the O···O distances are close to the experimental values for liquid water at 298 K (2.854 Å) [97-100] and hexagonal ice (I_h) at 183K (2.759 Å)

View Article Online
DOI: 10.1039/C9DT01922G

[101] as well as they fall in the range 2.70–2.94 Å obtained by quantum mechanical and semiempirical methods for four-membered water cycles [102- 107]. They are also well correlated with the values reported for other compounds containing tetramer assembly, including $\{[Co_2(bib)_2(fum)(HCOO)_2(H_2O)_2]\cdot 10H_2O\}_n$ (2.731 Å and 2.846 Å) [108], $[Co(phen)_3]S_4O_6\cdot 7H_2O$ (2.785 Å and 2.910 Å) [109], $[Ag_2(pda)(bipy)_2]_n\cdot 4nH_2O$ (2.775 Å and 2.793 Å) [110], $[Co_2(bta)(H_2O)_8]_n\cdot 4nH_2O$ (2.772 Å, 2.751 Å and 2.780 Å, 2.773 Å) [111], $[Cu(adipate)(4,4\text{-bipyridine})]\cdot(H_2O)_2$ (2.775 Å, 2.896 Å) [112], $[(Bpyph)(SCN)_2]\cdot 2H_2O$ (2.83 Å and 2.80 Å), $\{(HBpyph)[Fe(CN)_6]\}\cdot 5.5H_2O$ (2.69 Å and 2.76 Å) [113], $[Tc_4(CO)_{12}\text{-}(\mu_3\text{-}OH)_4\cdot 4H_2O]$ (2.940 Å) [114] and $\{[Ni(IP)(H_2O)_4]\cdot(2H_2O)(SO_4^{2-})\}$ (2.723 Å) [115].

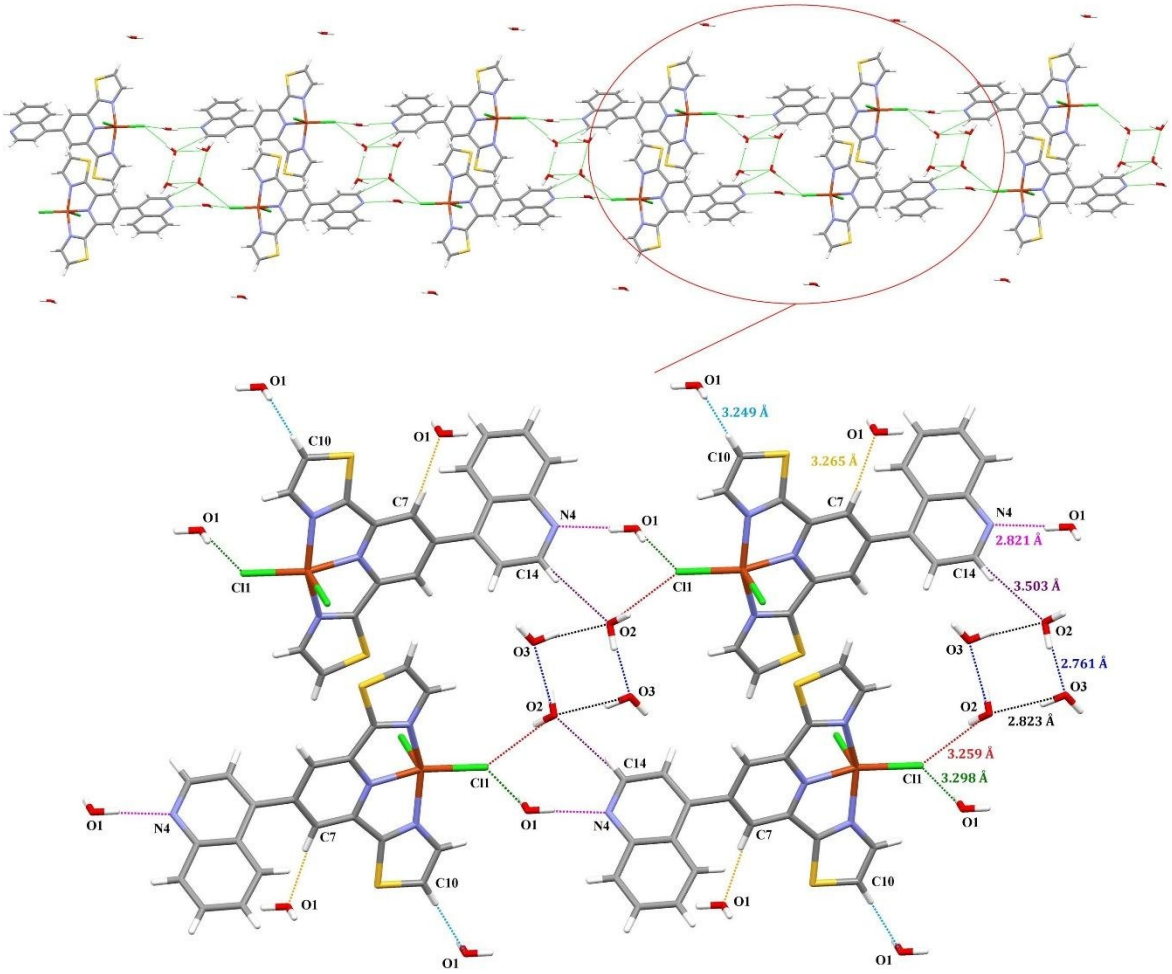

Fig. 3 Supramolecular double chains and hydrogen bonds involving water molecules in complex**4**.

The water tetramers are linked through O(2)—H(2A)•••Cl(1) with two complex molecules $[Cu(L^n)Cl_2]$ giving rise to the formation of a supramolecular double chains along $[11\bar{1}]$, additionally stabilized by O(1)—H(1B)•••Cl(1), O(1)—H(1A)•••N(4) and C(14)—H(14)•••O(2). The formed double chains are further interlinked into 3D network by C(2)—H(2)•••Cl(2) and O(3)—H(3A)•••Cl(2) hydrogen

View Article Online
DOI: 10.1039/C9DT01922G

bonds and π•••π interactions involving thiazole: Cg(S(1)/C(3)/N(1)/C(1)/C(2))•••Cg(S(1)/C(3)/N(1)/C(1)/C(2)) [-1-*x*,1-*y*,2-*z*]; Cg(S(1)/C(3)/N(1)/C(1)/C(2))•••Cg(S(2)/C(9)/N(3)/C(10)/C(11)) [-1+*x*,*y*,*z*]; Cg(S(2)/C(9)/N(3)/C(10)/C(11)) ••• Cg(S(2)/C(9)/N(3)/C(10)/C(11)) [-*x*,-*y*,2-*z*] and quinoline rings (Cg(N(4)/C(12)/C(13)/C(14)/C(15)/C(16)) ••• Cg(N(4)/C(12)/C(13)/C(14)/C(15)/C(16)) [-*x*,1-*y*,1-*z*] and Cg(N(4)/C(12)/C(13)/C(14)/C(15)/C(16)••• Cg(C(15)/C(16)/C(17)/C(18)/C(19)/C(20)) [1-*x*,1-*y*,1-*z*].

3.2 Cytotoxicity studies

The toxicity of the Cu(II) complexes **1-6** was evaluated in A2780 (ovarian cancer derived cell line), HCT116 (colorectal cancer derived cell line) and in normal dermal fibroblasts (Figs. 4 and 5). Dose response curves were obtained and the toxicity between the compounds was compared using the IC_{50} values (concentration that inhibits 50% of cell proliferation) for each complex in each cell line (Table 2).

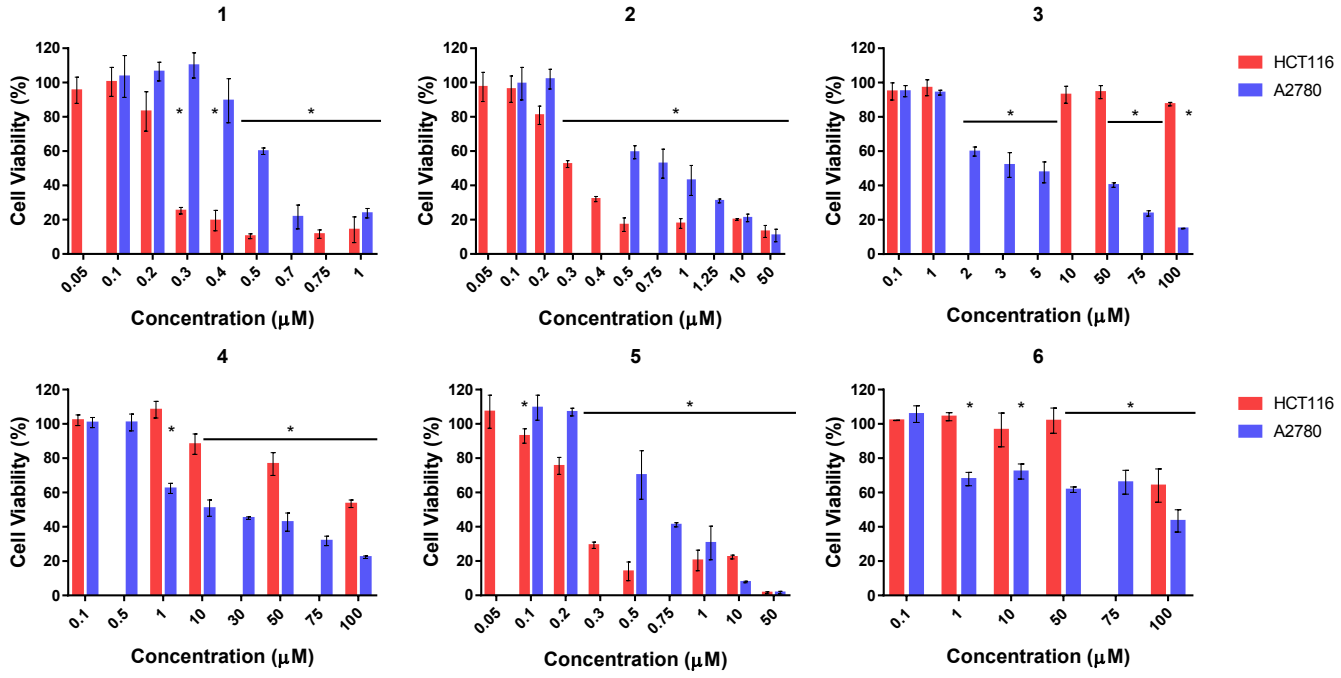

Fig. 4 Cytotoxicity of complexes **1-6** in HCT116 (red) and A2780 (blue) cancer cell lines. Cell viability was determined by the MTS method performed after 48 h of exposure to increasing concentrations of each complex. DMSO 0.1% (v/v) was used as solvent control. The results presented are mean ± SD of three independent assays. A p-value <0.05 is indicated by the symbol *.

View Article Online
DOI: 10.1039/C9DT01922G

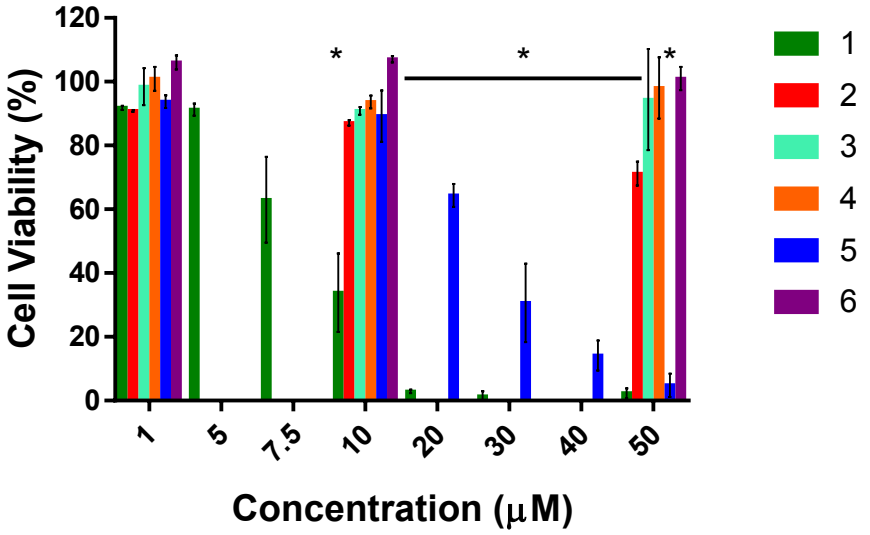

Fig. 5 Cytotoxicity of complexes **1**-**6** in human normal primary fibroblasts. evaluated after 48 h of exposure to increasing concentrations of each complex. Cell viability was determined by the MTS method. DMSO 0.1% (v/v) was used as solvent control condition. The results presented are mean ± SD of three independent assays. A p-value <0.05 is indicated by the symbol *.

Table 2 Values of relative IC_{50} (μM) of Cu(II) complexes **1**-**6** in HCT116 and A2780 cancer lines and in human normal dermal fibroblasts. The results presented are mean ± SD of three independent assays.

Cell lines	1 (μM)	2 (μM)	3 (μM)	4 (μM)	5 (μM)	6 (μM)
HCT116	0.3±0.09	0.3±0.06	>100	>100	0.2±0.08	>100
A2780	0.5±0.08	0.5±0.09	2.4±0.13	16.5±0.14	0.6±0.06	75<IC_{50}<100
Fibroblasts	9.4±0.02	>50	>50	>50	27.64±0.11	>50

Antiproliferative activities of the complexes followed the trend **1**~**2**~**5** > **3**~**4** > **6** in both cancer cell lines, HCT116 and A2780 (Fig. 3 and table 1). In fibroblasts, the trend was slightly different, **1** > **5** > **2**~**3**~**4**~**6**, with **2** and **6** showing antiproliferative effect (higher cell viability) than **1** and **5** (Fig. 4 and Table

View Article Online
DOI: 10.1039/C9DT01922G

1). The Cu(II) complexes with quinolyl-substituted 2,2′:6′,2″-terpyridines (terpy), **1** and **2**, showed to be the most active compared to other complexes in both cancer cell lines, HCT116 and A2780 (Figure 3 and Table 1). Less active were the Cu(II) complexes with quinolyl-substituted 2,6-di(thiazol-2-yl)pyridines (dtpy), complexes **3** and **4**, that displayed an antiproliferative effect only in the A2780 ovarian cancer cell line (Figs. 3 and 4 and Table 1). This specificity for the A2780 is corroborated by our previously results with other Cu(II) and Pt(II) complexes with different 4'-dtpy substitutions [65]. Interestingly, the loss of cell viability induced by Cu(II) complexes with ligands bearing quinol-2-yl moieties (**1** and **5**) is higher than that presented by the Cu(II) complexes bearing ligands with quinol-4-yl moieties (**2** and **6**) (Table 1). The Cu(II)quinolyl-2-yl-dppy, complex **5**, exhibited loss of cell viability similar to both Cu(II)terpy complexes, **1** and **2**, while the Cu(II)quinolyl-4-yl-dppy, complex **6**, presented no significative antiproliferative effect in none of the cell lines tested. It is possible to observe an effect of the quinolyl bond position on cytotoxicity within Cu(II)dtpy and Cu(II)dppy complexes in A2780 cell line and for the Cu(II)terpy complexes also in fibroblasts: the Cu(II) complexes with quinolyl-2-yl substitutions are more cytotoxic than the complexes with quinolyl-4-yl substitutions (Figures 3 and 4 and table 1).

Our previous work have shown a selective antiproliferative activity towards A2780 cell line of the Pt(II) and Cu(II) complexes with dtpy ligands [65]. Comparing the antiproliferative effect the Cu(II)quinolyl-2-yl-dtpy with other complexes with 4'-dtpy ligands already tested by us, it is possible to observe that this antiproliferative effect is similar in A2780, ranging from 2.4 μM (this report) to 11 μM [65]. Comparing metal complexes with terpy ligands in this report with others already published by us, the IC_{50} ranges from 0.27 μM (this report 0.3 μM, the lowest in Cu(II) complexes) to > 100 μM μM in the HCT116 cell line and in the A2780 cell line ranges from 0.5 μM (this report) to > 100 μM (Table 1) [101,65,116]. In normal human fibroblasts, metal complexes with terpy displayed cytotoxicity ranging from 0.3 μM to > 100 μM (Table 1) [65,116]. In this report, as well as in our previous works, it is possible to observe that the 4'-terpy substitution can attenuate the antiproliferative effect of the terpy ligand in fibroblasts (65, 82, 116, Table 1). The Cu(II)quinolyl-4-yl-terpy complex has a decreased cytotoxicity for normal human fibroblast cells while maintaining cytotoxicity towards both cancer cell lines tested, HCT116 and A2780 (Figs. 3 and 4 and Table 1).

Considering the higher antiproliferative effect in cancer cell lines and low activity in normal cells complexes **2** and **5** were selected for further biological studies in order to gain insights into the mechanisms that selectively reduce cancer cell line viability. HCT116 cells were incubated for 48 h with IC_{50} concentrations of either complex. Fluorescence microscopy of cells stained with Hoechst 33258 enable the observation of

View Article Online
DOI: 10.1039/C9DT01922G

cell nuclei and, if present, the identification of apoptotic bodies which result from the chromosome condensation and fragmentation (Fig. 5). These apoptotic bodies are a hallmark apoptosis in cells [65,116].

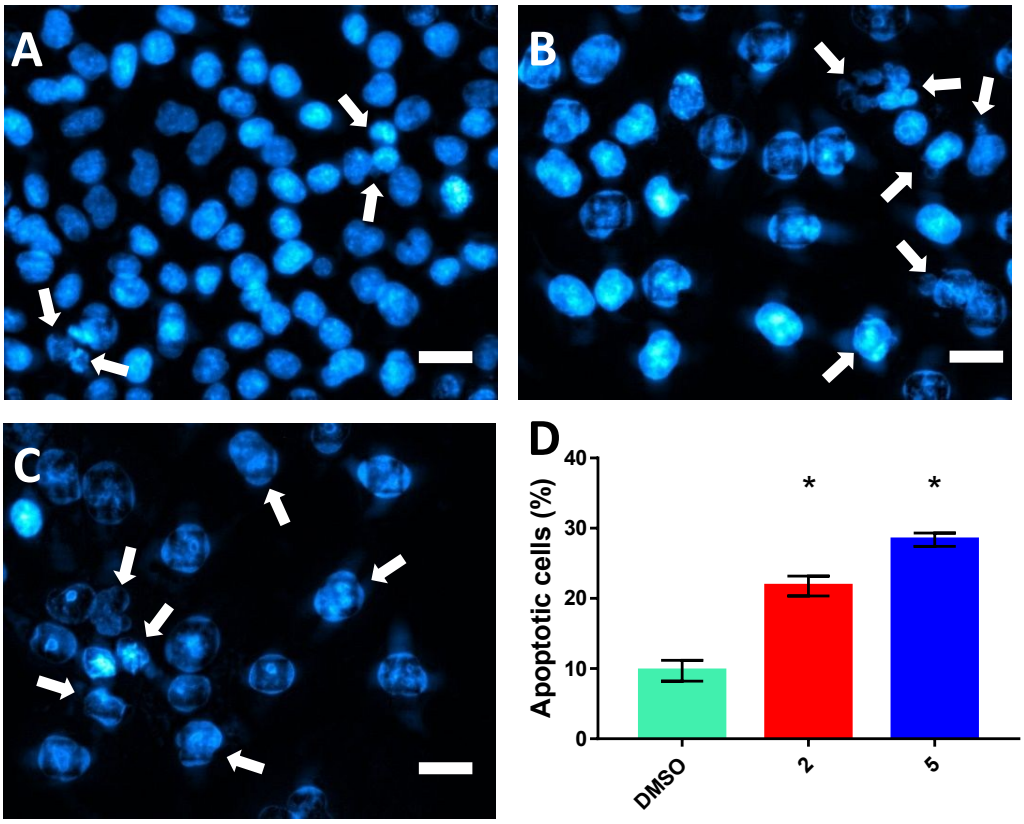

Fig. 6 Apoptosis induced after 48 h exposure of HCT116 cells to 0.1% (v/v) DMSO (A), IC_{50} concentration of (**2**) (B) and of (**3**) (C) evaluated by nuclei staining with Hoechst 33258. (D) % of apoptotic cells calculated based on the analysis of more than 5 different Hoechst fluorescence images for each condition. DMSO 0.1% (v/v) was used as solvent control. The symbol * indicates that the p-value < 0.001. Scale bars have a 20 µm length. White arrows indicate nuclei with apoptotic bodies.

It is possible to observe that exposure to both Cu(II) 4'-quinolyl-4-yl-terpy (**2**) and Cu(II) 4'quinolyl-2-yl-dppy (**5**) complexes increases the percentage of cells in apoptosis when compared to the control condition (Fig. 6). Apoptotic figures increase approximately 124 % and 192 % in cells treated with IC_{50} concentrations of **2** and **5**, respectively (Fig. 6). The results for complex **2** are in accordance with our previous published results for with other metal complexes with terpy and dtpy ligands [65,116]. The results

View Article Online
DOI: 10.1039/C9DT01922G

for the Cu(II) quinolyl-2yl-dppy complex (**5**), indicates that apoptosis may also play a role in the cytotoxicity of Cu(II) dppy complexes in cancer cells (Fig. 6).

One of the underlying mechanisms that can potentially trigger apoptosis in cancer cells is the increase in the production reactive oxygen species (ROS) [117]. For this reason, ROS production was investigated HCTT116 cells exposed for 48 h to IC_{50} concentrations of complexes **2** and **5** (Fig. 7).

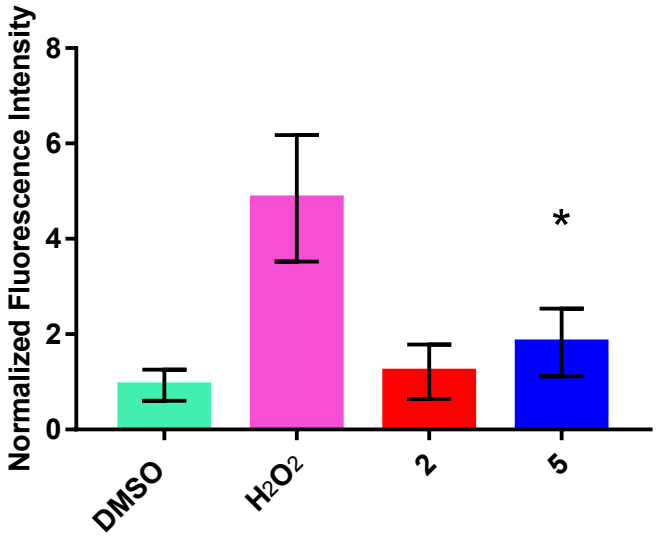

Fig. 7 Production of reactive oxygen species (ROS) in HCT116 cells exposed for 48 h to IC_{50} concentrations of complex **2** and **5**. DMSO 0.1% (v/v) was used as solvent control and 25 μM H_2O_2 was used as positive control. The symbol * indicates that the p-value ≤ 0.0001.

It is possible to observe a significant increase of 97% of ROS in HCT116 cells exposed to complex **5** when compared to the solvent control (Fig. 7). Although not statistically significant, an increase of 31% was also observed in HCT116 cells exposed to **2** (Fig. 7). In our previous published results, there was also a correlation between an increase in the percentage of apoptotic cells with increase in ROS in cells exposed to metal complexes with terpy ligands [65,116].

Our results show that Cu(II)terpy and Cu(II)dppy complexes have an antiproliferative potential against colorectal and ovarian carcinoma cells. The most cytotoxic are the terpy complexes. Some 4'terpy substitutions can alleviate toxicity for normal human fibroblasts. In particular, the 4'quinolyl-4-yl-terpy substitution significantly diminishes cytotoxicity in normal fibroblasts while maintaining cytotoxicity in

View Article Online
DOI: 10.1039/C9DT01922G

cancer cells (HCT116 and A2780) (Figs. 4 and 5 and Table 2). The dtpy complexes show a specificity towards the ovarian cancer derived cell line, A2780 (Figs. 4 and 5 and Table 2 and Ref. [65]. The Cu(II) quinolyl-2-yl-dppy complex, **5**, toxicity was associated with the increase in percentage of cells in apoptosis, an increase accompanied with higher levels of ROS in HCT116 cells (Figs. 6 and 7). Exposure of Cu(II) quinolyl-4-yl-terpy complex, **2**, displayed the ability to induce apoptosis in HCT116, an ability displayed by terpy metal complexes studied by our group regardless of the 4'terpy substitution (65, 116). Although the increase in ROS levels was not statistically significative for this terpy complex, a higher percentage of apoptotic cells are accompanied by higher levels of ROS in cells in other terpy complexes synthetized by our group [65,116].

2.3 Compounds 1-6 catalyze oxidations of alkanes and alcohols with hydroperoxides

In many cases, copper derivatives are known to efficiently catalyze the oxidation of hydrocarbons and alcohols with peroxides [118-131] affording alkyl hydroperoxides and ketones (aldehydes). Here, we have found that compounds **1-6** catalyze the oxidation of alkanes with H_2O_2 in acetonitrile. Accumulation of cyclohexanol and cyclohexanone (after reduction of reaction samples with PPh_3) in oxidation of cyclohexane with hydrogen peroxide catalyzed by compound **3** and **4** is demonstrated by Fig. 8.

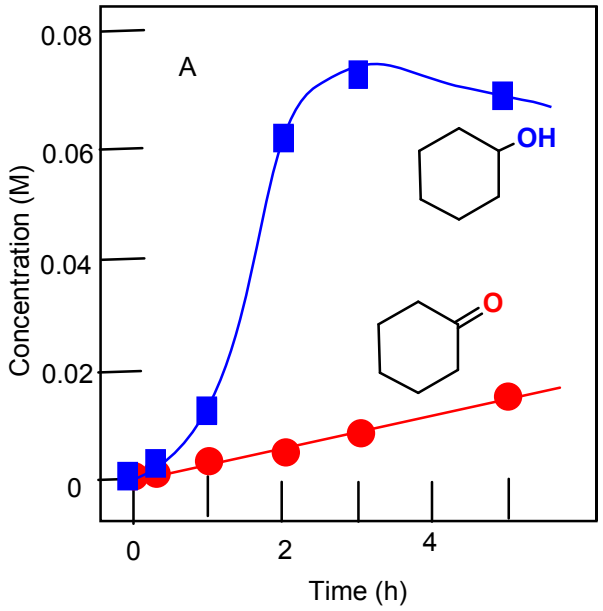

View Article Online
DOI: 10.1039/C9DT01922G

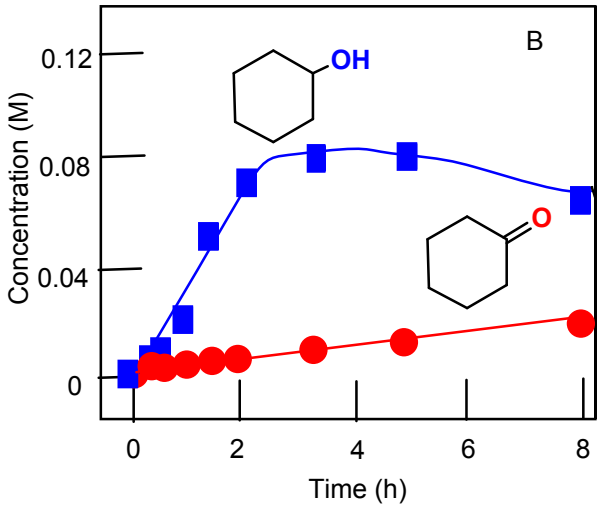

Fig. 8 Accumulation of cyclohexanol and cyclohexanone in oxidation of cyclohexane (0.46 M) with hydrogen peroxide (2.0 M, 50 % aqueous) catalyzed by compound **3** (graph A) and **4** (graph B)(concentration for all complexes 5×10^{-4} M) in MeCN at 50 °C. Concentrations of cyclohexanone and cyclohexanol were measured after reduction of the aliquots with solid PPh_3.

View Article Online
DOI: 10.1039/C9DT01922G

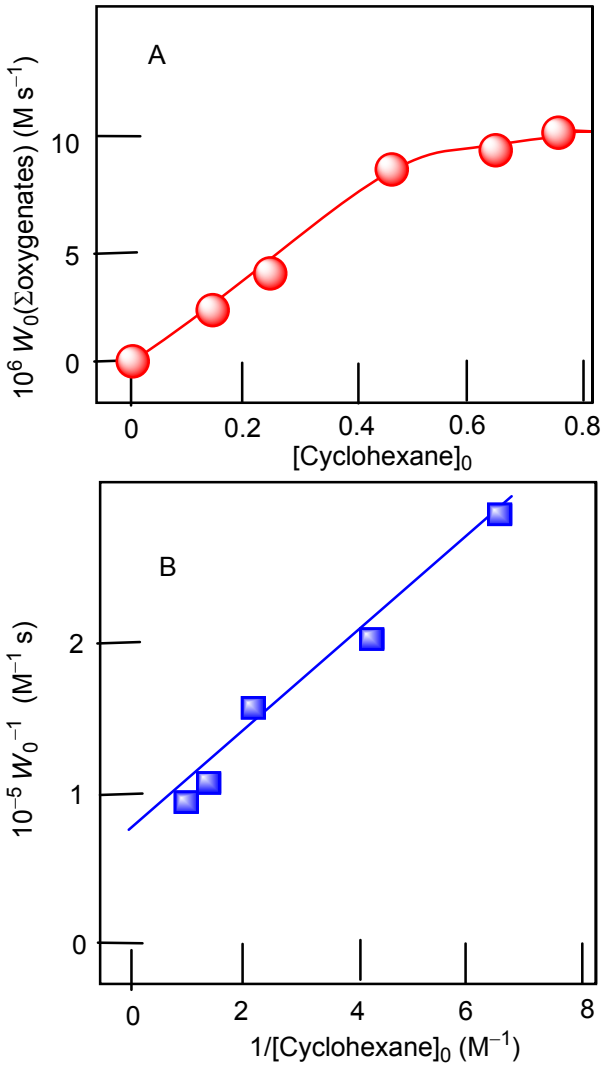

Fig. 9 Dependence of the initial rate of oxygenate formation W_0 on initial concentration of cyclohexane is shown in graph A. Linearization of the curve from graph A in coordinates $W_0^{-1} - 1/[C_6H_{12}]$ is presented in graph B. Concentrations of cyclohexanone and cyclohexanol were determined after reduction of the aliquots with solid PPh_3.

Earlier we studied the catalytic systems, based on the data on selectivity of alkane oxidation and we concluded that the oxidizing species is a hydroxyl radical. This conclusion has received kinetic confirmation [132]. We determined the ratio of the rate constants on the basis of experimental data within the framework of a model of competitive interaction of the generated by catalytic system species with acetonitrile on the one hand and cyclohexane on the other hand. These ratios were close to the value determined during the oxidation of cyclohexane in acetonitrile, when the species inducing oxidation is certainly a hydroxyl radical, arising from the photodissociation of H_2O_2 as the primary product [132].

The kinetic characteristics of the oxidizing species X generated by the catalytic system under discussion were obtained from the dependence of the alkane oxidation rate on its initial concentration (Fig.

View Article Online
DOI: 10.1039/C9DT01922G

9). The nature of the dependence corresponds to the assumption of the competitive interaction of the oxidizing species X with acetonitrile and cyclohexane (RH):

H_2O_2 + compound **1** → X (1)

X + CH_3CN →...→ products (2)

X + RH →...→ ROOH (3)

Here, stage (1) is the effective reaction of generating oxidizing species X at a rate of W_1; stages (2) and (3) are the transformations of CH_3CN and RH with the formation, in particular, of alkyl hydroperoxide ROOH, induced by interactions that limit their speed with X. The rate constants of these interactions are k_2 and k_3, respectively. If we assume that the concentration of species X is quasi-stationary, we obtain the following expression for the initial rate of formation of ROOH:

$$d[ROOH]/dt)_0 = W_1/(1 + k_2[CH_3CN]/k_3[RH]_0) \quad (4)$$

Equation (4) can be transformed into expression (5), convenient for the analysis of experimental data:

$$(d[ROOH]/dt)_0^{-1} = W_1^{-1}\times(1 + k_2[CH_3CN]/k_3[RH]_0) \quad (5)$$

The experimental data shown in Fig. 9 (graph A) are in accord with equation (5), which indicates the validity of the model of competitive interaction of species X with CH_3CN and RH. It follows from Fig. 9 (graph B) that $W_1 = 1.4 \times 10^{-5}$ M s^{-1} and $k_2/k_3 = 0.029$. The obtained value is noticeably different from the 0.006–0.01 ratio which characterized the reactions involving hydroxyl radicals [132-134].

The low selectivity in the oxidation of alkanes with X species obtained in the present work, is close to the selectivity found for reactions involving hydroxyl radicals (see Table 3). This indicates that hydroxyl radicals are generated in the catalytic systems studied in this work. Similar results were obtained earlier by us on the nature of the oxidizing species in the course of the decomposition of H_2O_2 catalyzed with the complex Cu_4Na_4 silsesquioxane (Table 3, Entry 2 Ref. [135]) and using aluminum nitrate (Table 3, Entry 7, Ref.[136].)

Table 3 Selectivity Parameters in H_2O_2 Oxidations of Alkanes by Certain Catalytic Systems [a]

		C(1):C(2):C(3):C(4)	1°:2°:3°	*trans*/*cis*	
Entry	Catalytic system	*n*-Heptane	MCH	*cis*-1,2-DMCH	*trans*-1,2-DMCH
1	Catalyst **4**	1.0:2.6:2.6:2.5	1.0:4.7:8.8	0.8	

View Article Online
DOI: 10.1039/C9DT01922G

2	Cu_4Na_4-silsesquioxane [b]	1.0:5.6:5.6:5.0	1:6:16	0.96	
3	VO_3^-/PCA [c]	1:6:7:5	1:9:37	0.75	0.80
4	hν [d]	1:10:7:6	1:2:6	0.90	1.00
5	$FeSO_4$ [d]	1:5:5:4.5		1.30	1.20
6	$Ni(ClO_4)_2/L$ [e]	1:6:7:6	1:7:15		
7	$Al(NO_3)_3$ [f]	1:5:5:5	1:6:23	0.80	0.80
8	$NaAuCl_4$ [g]	1:35:25:23	1:116:255		
9	$[Mn_2L_2(O)_3]^{2+}/MeCO_2H$ [h]	1:46:35:34	1:26:200	0.34	4.1

[a] Parameter C(1):C(2):C(3):C(4) is relative normalized (calculated taking into account the number of hydrogen atoms at each carbon) reactivities of hydrogen atoms at carbons 1, 2, 3 and 4 of the chain of *n*-heptane (in some cases this parameter was determined for *n*-octane instead of *n*-heptane). Parameter 1º:2º:3º is relative normalized reactivities of hydrogen atoms at primary, secondary and tertiary carbons of methylcyclohexane and isooctane. Parameter *trans*/*cis* is the ratio of isomers of *tert*-alcohols with mutual *trans*- and *cis*-orientation of the methyl groups formed in the oxidation of *cis*- and *trans*-1,2-dimethylcyclohexane. All parameters were measured after reduction of the reaction mixtures with triphenylphosphine before GC analysis and calculated based on the ratios of isomeric alcohols.
[b] Catalyst Cu_4Na_4 -silsesquioxane [135].
[c] For this system, see Ref. 136.
[d]. For this system, see Ref. 132. .
[e] *L* is 1,4,7-trimethyl-1,4,7-triazacyclononane. For this system, see: Ref. 137.
[f] For this system, see: Ref. 138.
[g] For this system, see Ref. 139.
[h] *L* is 1,4,7-trimethyl-1,4,7-triazacyclononane. For this system, see Refs. 140,141.

Assuming that the concentrations of acetonitrile and cyclohexane near the reaction centre differ from their concentrations in the solution volume [142-146] we can resolve the contradiction The obtained results indicate that the ratio of acetonitrile and cyclohexane concentrations inside the cluster of the catalytic particle (near the reaction center) exceeds their ratio in volume. Possibly, this difference is due to a higher concentration of both components inside a cavity in the catalyst globule. If so, the concentration in the case of small acetonitrile molecules, CH_3CN, is higher in comparison with concentration of the hydrophobic relatively voluminous cyclohexane molecules [142].

Alcohols can be transformed into corresponding ketones by the oxidation with *tert*-butyl hydroperoxide catalysed with complex **4** (see, for example, Fig. 10).

View Article Online
DOI: 10.1039/C9DT01922G

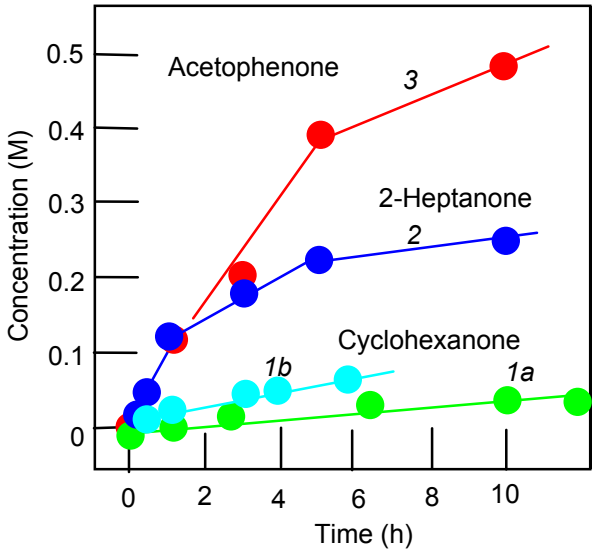

Fig. 10-Accumulation of cyclohexanone (curve *1*), 2-heptanone (curve 2) and acetophenone (curve *3*) in the oxidation of cyclohexanol (curve *1a*: 0.23 M; curve *1b*: 0.46 M), 2-heptanol (0.46 M) or 1-phenylethanol (0.5 M), respectively, with *tert*-butyl hydroperoxide (1.5 M) catalyzed by complex **4** (5×10^{-4} M) at 50 °C in acetonitrile. Concentrations of products were measured by GC after the reduction of the reaction sample with solid PPh_3.

3. Conclusions

In this work, structure–property relationship was investigated for a series of five-coordinate complexes $[CuCl_2(\kappa^3\text{-L})]$ bearing 2,2′:6′,2″-terpyridines (*terpy*), 2,6-di(thiazol-2-yl)pyridines (*dtpy*) and 2,6-di(pyrazin-2-yl)pyridines (*dppy*) functionalized with n-quinolyl substituents (n = 2 and 4). X-Ray analysis revealed striking difference in the relative orientation of the pendant substituent and central pyridine ring between the Cu(II) complexes bearing quinol-2-yl substituted ligands and those with quinol-4-yl group. While the quinol-4-yl unit was strongly inclined to the central pyridine of terpy, dtpy and dppy, the pendant substituent in the Cu(II) complexes bearing quinol-2-yl substituted ligands was quite coplanar with the central pyridine ring.

Cu(II)terpy and Cu(II)dppy complexes have an antiproliferative activity against colorectal and ovarian carcinoma cells with terpy complexes being the most antiproliferative in this cell line. 4'quinolyl-4-yl-terpy substitution significantly reduced the antiproliferative effect in normal fibroblasts while maintaining their effect in cancer cells (HCT116 and A2780). Dtpy complexes show a specificity towards A2780 cell line. The Cu(II) quinolyl-2-yl-dppy complex, **5**, was able to induce the loss of cell viability that correlated with an increase in the percentage of HCT116 cells in apoptosis and an increase in the levels of ROS. Exposure of Cu(II) quinolyl-4-yl-terpy complex, **2**, also displayed the ability to induce apoptosis in HCT116 but with a neglectful capability to induce ROS levels.

View Article Online
DOI: 10.1039/C9DT01922G

The first evaluation of compounds **1-6** in catalysis reveals that these complexes catalyze oxidation of alkanes into alkyl hydroperoxides with hydrogen peroxide as well as alcohols with *tert*-butyl hydroperoxide. A model of competitive interaction of hydroxyl radicals with CH_3CN and RH in the catalyst cavity has been proposed which is based on the study simultaneously of kinetics and selectivity in alkane oxidations. Analysis of the regioselectivity parameters found for the oxidation of linear and branched alkanes led the authors to a conclusion that the reaction mechanism includes the formation of hydroxyl radicals. The kinetic peculiarities of the cyclohexane oxidation with H_2O_2 in acetonitrile allowed us to assume that the oxidation proceeds in part in a cavity generated inside of the tris-heteroleptic copper cage.

Acknowledgement

The publication has been prepared with the support of the «RUDN University Program 5-100» and funded by RFBR according to Research Project Grant No. 19-03-00142, as well as by the Initiative Program (State registration number AAAA-A16-116020350251-6) in the frames of the State Tasks 0082-2014-0004 and 0082-2014-0007 “Fundamental regularities of heterogeneous and homogeneous catalysis”. This work was also performed within the framework of the Program of Fundamental Research of the Russian Academy of Sciences for 1013-2020 on the research issue of IChP RAS No. 47.16. State registration number of Center of Information Technologies and Systems for Executive Power Authorities (CITIS): AAAA-A17-117040610283-3. This work was supported by the Applied Molecular Biosciences Unit- UCIBIO which is financed by national funds from FCT/MCTES (UID/Multi/04378/2019). LRR acknowledges project PTDC/CVT/EPI/6685/2014.

No conflict of interest.

References

1. E. I. Solomon, D. E. Heppner, E. M. Johnston, J. W. Ginsbach, J. Cirera, M. Qayyum, M. T. Kieber-Emmons, C. H. Kjaergaard, R. G. Hadt and L. Tian, *Chem. Rev*. 2014, **114**, 3659−3853.

2. R. E. Cowleya, L. Tiana and E. I. Solomon, *PNAS October 25*, 2016, **113** (43) 12035-12040.

3. A. C Rosenzweig and M. H Sazinsky, *Current Opinion in Structural Biology*, 2006, **16,** 729–735.

4. L. Que Jr. and W. B. Tolman, *Nature*, 2008, **455**, 333-340.

5. A. M. Kirillov, M. V. Kirillova and A. J. L. Pombeiro, *Coord. Chem. Rev.*, 2012, **256,** 2741–2759.

6. S. Anbu, A. Paul, A. P. C. Ribeiro, M. F. C. Guedes da Silva, M. L. Kuznetsov and A. J. L. Pombeiro, *Inorg. Chim. Acta*, 2016, **450** 426-436.

View Article Online
DOI: 10.1039/C9DT01922G

7. R. Nasani, M. Saha, S. M. Mobin, L. M. D. R. S. Martins, A. J. L. Pombeiro, A. M. Kirillov and S. Mukhopadhyay, *Dalton Trans*., 2014, **43**, 9944–9954.
8. M. Sutradhar, T. R. Barman, A. J. L. Pombeiro and L. M. D. R. S. Martins, *Molecules*, 2019, **24**, 47.
9. M. Nandi and P. Roy, *Ind. J. Chem*., 2013, **52A,** 1263-1268.
10. T. Matsumoto, H. Furutachi, M. Kobino, M. Tomii, S. Nagatomo, T. Tosha, T.Osako, S. Fujinami, S. Itoh, T. Kitagawa and M. Suzuki, *J. Am. Chem. Soc.*, 2006, **128** (12), 3874-3875.
11. S. Kumar, S. Bawa and H. Gupta, *Mini-Rev. Med. Chem*., 2009, **9**, 1648–1654.
12. K. Kaur, M. Jain, R. P. Reddy and R. Jain, *Eur. J. Med. Chem.,* 2010, **45**, 3245–3264.
13. R. Musiol, M. Serda, S. Hensel-Bielowka and J. Polanski, *Curr. Med. Chem.,* 2010, **17**, 1960–1973.
14. V. R. Solomon and H. Lee, *Curr. Med. Chem.,* 2011, **18**, 1488–1508.
15. A. Marella, O. P. Tanwar, R. Saha, M. R. Ali, S. Srivastava, M. Akhter, M. Shaquiquzzaman and M. M. Alam, *Saudi Pharm. J*., 2013, **21**, 1–12.
16. S. Vandekerckhove and M. D'hooghe, *Bioorg. Med. Chem*., 2015, **23**, 5098–5119.
17. O. Afzal, S. Kumar, M. R. Haider, M. R. Ali, R. Kumar, M. Jaggi and S. Bawa, *Eur. J. Med. Chem.*, 2015, **97**, 871–910.
18. S. Jain, V. Chandra, P. K. Jain, K. Pathak, D. Pathak and A. Vaidya, *Arabian J. Chem.*, 2016, DOI:10.1016/j.arabjc.2016.10.009.
19. R. A. Alderden, M. D. Hall and T. W. Hambley, *J. Chem. Educ.*, 2006, **83**, 728734.
20. S. Dasari and P. B. Tchounwou, *Eur. J. Pharmacol*., 2014, **740**, 364–378.
21. D. A. Fennell, Y. Summers, J. Cadranel, T. Benepal, D. C. Christoph, R. Lal, M. Das, F. Maxwell, C. Visseren-Grul and D. Ferry, *Canc. Treat. Rev.,* 2014, **44**, 42–50.
22. M. Taylor and A. Filby, *Johnson Matthey Technol. Rev*., 2017, **61**, 32–39.
23. L. Cheng, P. Albers, D. M. Berney, D. R. Feldman, G. Daugaard, T. Gilligan and L. H. J. Looijenga, *Nat. Rev. Dis. Primers*., 2018, **4**, 29.
24. M. A. Fuertes, C. Alonso and J. M. Pérez, *Chem. Rev.*, 2003, **103**, 645–662.
25. D. Wang and S. J. Lippard, *Nat. Rev. Drug Discov.*, 2005, **4**, 307–320.
26. L. Kelland, *Nat. Rev. Cancer*, 2007, **7**, 573–584.
27. R. Oun, Y. E. Moussa and N. J. Wheate, *Dalton Trans.*, 2018, **47**, 6645–6653.
28. S. J. Lippard and J. M. Berg, *Principles of bioinorganic chemistry*, University Science Books, California, 1994.
29. I. Ott and R. Gust, *Arch. Pharm. (Weinheim)*, 2007, **340**, 117–126.
30. A. A. Holder, *Annu. Rep. Sect. Inorg. Chem.*, 2010, **106**, 504–525.
31. N. P. E. Barry and P. J. Sadler, *Chem. Commun.*, 2013, **49**, 5106–5131.
32. M. Zaki, F. Arjmand and S. Tabassum, *Inorg. Chim. Acta*, 2016, **444**, 1–22.

View Article Online
DOI: 10.1039/C9DT01922G

33. W. A. Wani, U. Baig, S. Shreaz, R. A. Shiekh, Prince F. Iqbal, E. Jameel, A. Ahmad, S. H. Mohd-Setapar, M. Mushtaqueh and L. T. Hun, *New J. Chem.*, 2016, **40**, 1063–1090.

34. R. Tabti, N. Tounsi, C. Gaiddon, E. Bentouhami and L. Désaubry, *Med. Chem.*, 2017, **7**, 875–879.

35. U. Ndagi, N. Mhlongo and M. E. Soliman, *Drug Des. Devel. Ther.*, 2017, **11**, 599–616.

36. Y. Ellahioui, S. Prashar and S. Gómez-Ruiz, *Inorganics*, 2017, **5**, 4.

37. E. Alessio and Z. Guo, *Eur. J. Inorg. Chem.*, 2017, 1539–1540.

38. P. Pedrosa, A. Carvalho, P. V. Baptista and A. R. Fernandes, in *Basic Concepts Viewed from Frontier in Inorganic Coordination Chemistry,* ed. Takashiro Akitsu, IntechOpen, 2018, chapter: *Inorganic Coordination Chemistry: where we stand in cancer treatment?*

39. E. M. Domínguez-Martís, D. G. Mosteiro-Miguéns, L. Vigo-Gendre, D. López-Ares, M. Freire-Garabal, M. J. Núñez-Iglesias and S. Novío, *Crystals*, 2018, **10**, 369;

40. K. G. Daniel, D. Chen, B. Yan, Q. P. Dou, *Front Biosci*., 2007, **12**, 135–144;

41. F. Tisato, C. Marzano, M. Porchia, M. Pellei and C. Santini, *Med. Res. Rev.*, 2010, **30**, 708–749.

42. J. Nelson, *Annu. Rep. Sect. Inorg. Chem.*, 2010, **106**, 235–254.

43. D. Denoyer, S. Masaldan, S. La Fontaine and M. A. Cater, *Metallomics,* 2015, **7**, 1459–1476.

44. W. Zheng, Y. Zhao, Q. Luo, Y. Zhang, K. Wu and F. Wang, *Curr. Top. Med. Chem.,* 2017, **17**, 3084–3098.

45. C. Marzano, M. Pellei, F. Tisato and C. Santini, *Anticancer Agents Med. Chem*., 2009, **9**, 185–211.

46. C. Santini, M. Pellei, V. Gandin, M. Porchia, F. Tisato and C. Marzano, *Chem. Rev.*, 2014, **114**, 815–862.

47. R. Tabti, N. Tounsi, C. Gaiddon, E. Bentouhami and L. Désaubry, *Med. Chem.*, 2017, **7**, 875–879.

48. T. J. P. McGivern, S. Afsharpour and C. J. Marmion, *Inorganica Chim. Acta*, 2018, **472**, 12–39.

49. C. Shobha Devi, B. Thulasiram, R. R. Aerva and P. Nagababu, *J. Fluoresc.,* 2018, **28**, 1195–1205.

50. D. Denoyer, S. A. S. Clatworthy and M. A. Cater, in *Metallo-Drugs: Development and Action of Anticancer Agents*, ed. A. Sigel, H. Sigel, E. Freisinger, R. K. O. Sigel, De Gruyter, Berlin, Boston, 2018, chapter 16. Copper Complexes in Cancer Therapy, pp. 469-506.

51. V. M. Manikandamathavan, V. Rajapandian, A. J. Freddy, T. Weyhermüller, V. Subramanian and B. U. Nair, *Eur. J. Med. Chem.*, 2012, **57**, 449–458.

View Article Online
DOI: 10.1039/C9DT01922G

52. S. Rajalakshmi, T. Weyhermüller, M. Dinesh and B. U. Nair, *Journal of Inorganic Biochemistry*, 2012, **117**, 48–59.

53. W. Chu, Y. Wang, S. Liu, X. Yang, S. Wang, S. Li, G. Zhou, X. Qin, C. Zhou and J. Zhang, *Bioorg. Med. Chem. Lett.*, 2013, **23**, 5187–5191.

54. [36] J.-W. Liang, Y. Wang, K.-J. Du, G.-Y. Li, R.-L. Guan, L.-N. Ji and H. Chao, *J. Inorg. Biochem.*, 2014, **141**, 17–27.

55. V. M. Manikandamathavan, M. Thangaraj, T. Weyhermuller, R. P. Parameswari, V. Punitha, N. N. Murthy and B. U. Nair, *Eur. J. Med. Chem.*, 2017, **135**, 434–446.

56. K. Tummalapalli, C. S. Vasavi, P. Munusami, M. Pathak and M. M. Balamurali, *Int. J. Biol. Macromol.*, 2017, **95**, 1254–1266.

57. D.-Y. Zhang, Y. Nie, H. Sang, J.-J. Suo, Z.-J. Li, W. Gu, J.-L. Tian, X. Liu and S.-P. Yan, *Inorg. Chimica Acta*, 2017, **457**, 7–18.

58. B. Deka, T. Sarkar, S. Banerjee, A. Kumar, S. Mukherjee, S. Deka, K. K. Saikia and A. Hussain, *Dalton Trans.,* 2017, **46**, 396–409.

59. B. Deka, A. Bhattacharyya, S. Mukherjee, T. Sarkar, K. Soni, S. Banerjee, K. K. Saikia, S. Deka and A. Hussain, *Appl. Organometal. Chem*. 2018, **32**, e4287.

60. B. Đ. Glišić, J. Nikodinovic-Runic, T. Ilic-Tomic, H. Wadepohl, A. Veselinović, I. M. Opsenica and M. I. Djuran, *Polyhedron*, 2018, **139**, 313–322.

61. D. Maheshwaran, T. Nagendraraj, P. Manimaran, B. Ashokkumar, M. Kumar and R. Mayilmurugan, *Eur. J. Inorg. Chem.*, 2017, **6,** 1007–1016.

62. Z. Ma, L. Wei, E. C. B. A. Alegria, L. M. D. R. S. Martins, M. F. C. G. da Silva and A. J. L. Pombeiro, *Dalton Trans*., 2014, **43**, 4048–4058.

63. G. Zhang, E. Liu, C. Yang, L. Li, J. A. Golen and A. L. Rheingold, *Eur. J. Inorg. Chem*., 2015, **6,** 939–947.

64. A. Paul, A. P. C. Ribeiro, A. Karmakar, M. F. C. G. da Silva and A. J. L. Pombeiro, *Dalton Trans*., 2016, **45**, 12779–12789.

65. K. Czerwińska, B. Machura, S. Kula, S. Krompiec, K. Erfurt, C. Roma-Rodrigues, A. R. Fernandes, L. S. Shul'pina, N. S. Ikonnikov and G. B. Shul'pin, *Dalton Trans.*, 2017, **46**, 9591–9604.

66. S. Blanchard, E. Derat, M. Desage-El Murr, L. Fensterbank, M. Malacria and V. Mouriès-Mansuy, *Eur. J. Inorg. Chem.* **2012, 3**, 376–389.

67. M. Mitra and A. A. Shteinman, *J. Applicable Chem.*, 2018, **7** (2), 417-425.

68. W. Kaim, *Eur. J. Inorg. Chem.* 2012, 343–348.

View Article Online
DOI: 10.1039/C9DT01922G

69. M. Yu, M. B. Ward, A. Franke, S. L. Ambrose, Z. L. Whaley, T. M. Bradford, J. D. Gorden, R. J. Beyers, R. C. Cattley, I. Ivanović-Burmazović, D. D. Schwartz and C. R Goldsmith, *Inorg. Chem.*, 2017, **56**, 2812-2826.

70. C. Römelt, T. Weyhermüller, K. Wieghardt, *Coordination Chemistry Reviews,* 2019, **380**, 287–317

71. K. T. Mahmudov, book , Noncovalent interactions in catalysis.

72. K. T. Mahmudov, A. V. Gurbanov, F. I. Guseinov and M. F. C. Guedes da Silva, *Coord. Chem. Rev.*, 2019, **387,** 32–46

73. A. Maroń, A. Szlapa, T. Klemens, S. Kula, B. Machura, S. Krompiec, J. G. Małecki, A. Świtlicka-Olszewska, K. Erfurt and A. Chrobok, *Org. Biomol. Chem*., 2016, **14**, 3793–3808.

74. T. Klemens, A. Świtlicka-Olszewska, B. Machura, M. Grucela, E. Schab-Balcerzak, K. Smolarek, S. Mackowski, A. Szlapa, S. Kula, S. Krompiec, P. Lodowski and A. Chrobok, *Dalton Trans.,* 2016, **45**, 1746–1762.

75. A. Maroń, S. Kula, A. Szlapa-Kula, A. Świtlicka, B. Machura, S. Krompiec, J. G. Małecki, R. Kruszyński, A. Chrobok, E. Schab-Balcerzak, S. Kotowicz, M. Siwy, K. Smolarek, S. Maćkowski, H. Janeczek and M. Libera, *Eur J. Org. Chem.,* 2017, **19**, 2730–2745.

76. Oxford Diffraction. CrysAlis PRO., Oxford Diffraction Ltd, Yarnton, England, 2011.

77. G. M. Sheldrick, *Acta Cryst. A,* 2008, **64**, 112–122.

78. G. M. Sheldrick, *Acta Cryst C*, 2015, **71**, 3–8.

79. T. F. S. Silva, P. Smoleński, L. M.D.R.S. Martins, M. F. Guedes da Silva, A. R. Fernandes, D., A. Silva, S. Santos, P. M. Borralho, C. M. P. Rodrigues and A. J. L. Pombeiro, *Eur J Inorg Chem.,* 2013; **21**, 3651-3658..

80. T. F. S. Silva, L. M. D. R. S. Martins, M. F. Guedes da Silva, M. L. Kuznetsov, A. R. Fernandes, A. Silva, C-J. Pan, J-F. Lee, B-J. Hwang and A. J. L. Pombeiro. *Chemistry – an Asian J.* 2014; **9**, 1132-1143.

81. M. Sutradhar, A. R. Fernandes, F. Paradinha, P. Rijo, C. Garcia, C. Roma- Rodrigues, A. J. L. Pombeiro and A. J. Charmier, *J Inorg Biochem*, 2019, **190**, 31-37.

82. A. Maroń, K. Czerwińska, B. Machura, L. Raposo, C. Roma-Rodrigues, A. R. Fernandes, J. G. Małecki, A. Szlapa-Kula, S. Kula, S. Krompiec, *Dalton Trans*., 2018, **47**, 6444- 6463.

83. N. Svahn, A. J. Moro, C. Roma-Rodrigues, R. Puttreddy, K. Rissanen, P. V. Baptista, A. R. Fernandes, J. C. Lima and L. Rodriguez, *Chemistry*, 2018, **24**, 14654-14667.

84. K. Das, B. B. Beyene, A. Datta, E. Garribba, C. Roma-Rodrigues, A. Silva, A. R. Fernandes and C. H. Hung, *New J. Chem.*, 2018, **42**, 9126-9139.

View Article Online
DOI: 10.1039/C9DT01922G

85. G. B. Shul'pin, *J. Mol. Catal. A*: *Chem*., 2002, **189,** 39–66.

86. G. B. Shul'pin, *Comptes Rendus, Chimie,* 2003, **6,** 163–178.

87. G. B. Shul'pin, Y. N. Kozlov, L. S. Shul'pina, A. R. Kudinov and D.Mandelli, *Inorg. Chem.,* 2009, **48,** 10480–10482.

88. G. B. Shul'pin, Y. N. Kozlov, L.S. Shul'pina and P. V. Petrovskiy, *Appl. Organometal. Chem.*, 2010, **24,** 464–472.

89. G. Olivo, O. Lanzalunga and S. Di Stefano, (Review). *Adv. Synth. Catal*. 2016, **358**, 843–863.

90. I. Garcia-Bosch and M. A. Siegel, *Angew. Chem., Int. Ed*., 2016, **55**(41), 12873–12876.

91. A. L. Maksimov, Y. S. Kardasheva, V. V. Predeina,. M. V. Kluev, D. N. Ramazanov, M.Y. Talanova and E. A. Karakhanov, *Petroleum Chem*., 2012, **52**(5) 318-326.

92. J. Wang and G. S. Hanan, *Synlett*, 2005, 1251–1254.

93. E. C. Constable, E. L. Dunphy, C. E. Housecroft, M. Neuburger, S. Schaffner, F. Schaper and S. R. Batten, *Dalton Trans*., 2007, 4323–4332.

94. A. N. Kharat, A. Bakhoda and S. Zamanian, *Polyhedron*, 2011, **30**, 1134–1142.

95. A. W. Addison, T. N. Rao, J. Reedijk, J. van Rijn and G. C. Verschoor, *J. Chem. Soc., Dalton Trans.,* 1984, 1349–1356

96. A. B. P. Lever*, Inorganic electronic spectroscopy*, Elsevier, Amsterdam, 1986.

97. A. H. Narten, W. E. Thissen and L. Blum, *Science*, 1982, **217**, 1033–1034.

98. J. K. Gregory, D. C. Clary, K. Liu, M. G. Brown and R. J. Saykally, *Science,* 1997, **275**, 814–817.

99. G. A. Jeffrey, *An Introduction to Hydrogen Bonding*, Oxford University Press, Oxford, 1997.

100. N. Keutsch and R. J. Saykally, *Proc. Natl. Acad. Sci. USA*, 2001, **98**, 10533–10540.

101. S. W. Peterson and H. A. Levy, *Acta Crystallogr*., 1957, **10**, 70–76.

102. S. S. Xantheas and T. H. Dunning Jr., *J. Chem. Phys*., 1993, **99**, 8774–8792.

103. S. S. Xantheas*, J. Chem. Phys*., 1994, **100**, 7523– 7534.

104. S. S. Xantheas, *J. Chem. Phys*., 1995, **102**, 4505–4517.

105. R. Ludwig, *Angew. Chem. Int. Ed.,* 2001, **40**, 1808–1827.

106. M. Masella, N. Gresh and J.-P. Flament, *J. Chem. Soc. Faraday Trans.,* 1998, **94**, 2745–2753.

107. J. Dolenc and J. Koller, *Acta Chim. Slov*., 2006, **53**, 229–237.

108. J. Wu and J.-Q. Liu, *Inorg. Chim. Acta*, 2013, **402**, 20–24.

109. R. P. Sharma, A. Singh, P. Venugopalan, P. Brandão and V. Félix, *Polyhedron*, 2012, **40**, 175–184.

View Article Online
DOI: 10.1039/C9DT01922G

110. G.-P. Yang, Y.-Y. Wang, P. Liu, A.-Y. Fu, Y.-N. Zhang, J.-C. Jin and Q.-Z. Shi, *Cryst. Growth Des.*, 2010, **10**, 1443–1450.

111. O. Fabelo, J. Pasán, L. Cañadillas-Delgado, F. S. Delgado, A. Labrador, F. Lloret, M. Julve and C. Ruiz-Pérez, *CrystEngComm*, 2008, **10**, 1743–1746.

112. L.-S. Long, Y.-R. Wu, R.-B. Huang and L.-S. Zheng, *Inorg. Chem.,* 2004, **43**, 3798–3800.

113. Y. Sun, J. Zhang, Z. Ju and G.-Y. Yang, *Aust. J. Chem.,* 2005, **58**, 572.

114. M. Zuhayra, W. U. Kampen, E. Henze, Z. Soti, L. Zsolnai, G. Huttner and F. Oberdorfer, *J. Am. Chem. Soc.,* 2006, **128**, 424–425.

115. H. Wang, J.-Q. Liu, Y.-N. Zhang, Y.-Y. Wang, G.-L. Wen, C.-Y. Guo, and Q.-Z. Shi, *Inorg. Chem. Commun*., 2008, **11**, 129–133.

116. A. Maroń, K. Czerwińska, B. Machura, L. Raposo, C. Roma-Rodrigues, A. R. Fernandes, J. G Małecki, A. Szlapa-Kula, S. Kula, S. Krompiec, *Dalton Trans*., 2018, **47**, 6444- 6463.

117. C. Giovannini, P. Matarrese, B. Scazzocchio, M. Sanchez, R. Masella, W. Malorni. *FEBS Letters*, 2002, **523**, 200-206.

118. E. T. Denisov and I. B. Afanas'ev, *Oxidation and Antioxidants in Organic Chemistry and Biology*, Taylor and Francis, CRC Press, 2005.

119. G. B. Shul'pin, *Organic Reactions catalyzed by Metal Complexes* (in Russian), URSS, Moscow, 2019.

120. A. K. Kirillov, M. V. Kirillova and A. J. L. Pombeiro, *Coord. Chem. Rev*., 2012, **256,** 2741-2759.

121. *Homogeneous Catalysis and Mechanisms in Water and Biphasic Media*, Editor L. Gonsalvi, MDPI, Basel, 2019.

122. A. N. Bilyachenko, M. M. Levitsky, A. I. Yalymov, A. A. Korlyukov, V. N. Khrustalev, A. V. Vologzhanina, L. S. Shul'pina, N. S. Ikonnikov, A. L. Trigub, P. V. Dorovatovskii, X. Bantreil, F. Lamaty, J. Long, J. Larionova, I. E. Golub, E. S. Shubina and G. B. Shul'pin, *Angew. Chem. Int. Ed.*, 2016, **55**, 15360-15363.

123. A. N. Kulakova, A. N. Bilyachenko, A. A. Korlyukov, J. Long, M. M. Levitsky, E. S. Shubina, Y. Guari and J. Larionova, *Dalton Trans*., 2018, **47**, 6893-6897.

124. A. N. Bilyachenko, V. N. Khrustalev, Y. V. Zubavichus, L. S. Shul'pina, A. N. Kulakova, X. Bantreil, F. Lamaty, M. M. Levitsky, E. I. Gutsul, E. S. Shubina and G. B. Shul'pin, *Inorg. Chem*., 2018, **57**, 528–534.

125. M. M. Levitsky, A. N. Bilyachenko and G. B. Shul'pin, *J. Organomet. Chem*., 2017, 849–850, 201-218.

126. A. N. Kulakova, A. A. Korlyukov, Y. V. Zubavichus, V. N. Khrustalev, X. Bantreil, L. S. Shul'pina, M. M. Levitsky, N. S. Ikonnikov, E. S. Shubina, F. Lamaty, A. N. Bilyachenko and G. B. Shul'pin, *J. Organomet. Chem*., 2019, **884**, 17-28.

127. A. P. Sadimenko and S. S. Basson, *Coord. Chem. Rev*., 1996, **147,** 247.

View Article Online
DOI: 10.1039/C9DT01922G

128. Y. Perez, R. Ballesteros, M. Fajardo, I. Sierra and I. del Hierro, *J. Mol. Catal. A: Chem.,* 2012, **352,** 45–56.
129. A. M. Kirillov, M. V. Kirillova, L. S. Shul'pina, P. J. Figiel, K. R. Gruenwald, M. F. C. Guedes da Silva, M. Haukka, A. J. L. Pombeiro and G. B. Shul'pin, *J. Mol. Catal. A: Chem.*, 2011, **350,** 26–34.
130. M. V. Kirillova, A. M. Kirillov, D. Mandelli, W. A. Carvalho, A. J. L. Pombeiro and G. B. Shul'pin, *J. Catal.*, 2010, **272,** 9–17.
131. N. Zhao, Y. Li, J. Gu, T. A. Fernandes, M. V. Kirillova and A. M. Kirillov, *Molecules*, 2019, **24**, 6.
132. G. B. Shul'pin, G. V. Nizova, Y. N. Kozlov, L. Gonzalez Cuervo and G. Süss-Fink, *Adv. Synth. Catal.*, 2004, **346** (2–3), 317–332.
133. D. S. Nesterov, E. N. Chygorin, V. N. Kokozay, V. V. Bon, R. Boča, Y. N. Kozlov, L. S. Shul'pina, J. Jezierska, A. Ozarowski, A. J. L. Pombeiro and G. B. Shul'pin, *Inorg. Chem*., 2012, **51**(16), 9110–9122.

134. G. B. Shul'pin, D. S. Nesterov, L .S. Shul'pina and A. J. L. Pombeiro, *Inorg. Chim. Acta*, 2017, **455**, 666-676.

135. A. N. Kulakova, V. N Khrustalev, Y. V Zubavichus, L. S Shul'pina, E. S Shubina, M. M Levitsky, N. S Ikonnikov, A. N Bilyachenko, Y. N Kozlov and G. B Shul'pin, *Catalysts,* 2019, **9** (2), paper 154.
136. G. B. Shul'pin, Y. N. Kozlov, G. V. Nizova, G. Süss-Fink, S. Stanislas, A. Kitaygorodskiy and V. S. Kulikova, *J. Chem. Soc., Perkin Trans. 2,* 2001, 1351–1371.
137. G. B. Shul'pin, *J. Chem. Res. (S)* 2002, 351–353.

138. D. Mandelli, K. C. Chiacchio, Y. N. Kozlov and G. B. Shul'pin, *Tetrahedron Lett.*, 2008, **49**, 6693–6697.

139. G. B. Shul'pin, G. Süss-Fink and A. E. Shilov, *Tetrahedron Lett*., 2001, **42**, 7253–7256.
140. G. B. Shul'pin, M. G. Matthes, V. B. Romakh, M. I. F. Barbosa, J. L. T. Aoyagi and D.Mandelli, *Tetrahedron*, 2008, **64**, 2143–2152.
141. G. B. Shul'pin, Y. N. Kozlov, S. N. Kholuiskaya and M. I. Plieva, *J. Mol. Catal. A: Chem*., 2009, **299**, 77–87.
142. G. B. Shul'pin (Review), *Catalysts*, 2016, **6**(4), paper No. 50.

143. I. P. Beletskaya and V. Tyurin, *Molecules,* 2010, **15**, 4792-4814.

144. G. B. Shul'pin, (Review), *Org. Biomol. Chem*. 2010, **8**, 4217–4228.

145. G. B. Shul'pin, Perspective, *Dalton Trans*., 2013, **42**(36), 12794–12818.

146. G. B. Shul'pin, "Selectivity in C–H functionalizations", in: J. Reedijk, K. Poeppelmeier, L. Casella (Eds), *Comprehensive Inorganic Chemistry II*, 2nd Edition, Vol. 6, Chapter 6.04, Elsevier, 2013, pp. 79–104.

Copper(II) complexes with 2,2':6',2"-terpyridine, 2,6-di(thiazol-2-yl)pyridine and 2,6-di(pyrazin-2-yl)pyridine substituted with quinolines. Synthesis, structure, antiproliferative activity, and catalytic activity in oxidation of alkanes and alcohols with peroxides †

Katarzyna Choroba,[a] Barbara Machura,*[a] Slawomir Kula,[a] Luis R. Raposo,[b] Alexandra R. Fernandes,*[b]

Rafal Kruszynski,[c] Karol Erfurt,[d] Lidia S. Shul'pina,[e] Yuriy N. Kozlov [f,e] and Georgiy B. Shul'pin *[f,g,h]

View Article Online
DOI: 10.1039/C9DT01922G

Graphical Abstract for Dalton Trans.

The toxicity of six new Cu(II) complexes was evaluated HCT116 (colorectal cancer derived cell line) and in A2780 (ovarian cancer derived cell line). A model of competitive interaction of hydroxyl radicals with CH_3CN and RH in the catalyst cavity has been proposed which is based on the study simultaneously of kinetics and selectivity in alkane oxidations.